THE RELATIONSHIP BETWEEN CHOLINERGIC AND NORADRENERGIC ACTIVITY AND BEHAVIORAL STATE

by

JOHN JOSEPH FRANCIS

A THESIS

Presented to the Department of Biology
and the Robert D. Clark Honors College
in partial fulfillment of the requirements for the degree of
Bachelor of Science

May 2021

An Abstract of the Thesis of

John Joseph Francis for the degree of Bachelor of Science
in the Department of Biology to be taken June 2021

Title: The Relationship Between Cholinergic and Noradrenergic Activity and Behavioral State

Approved: _____*David McCormick, Ph.D.*____
Primary Thesis Advisor

Approved: _____*Lindsay Collins, Ph.D.*_____
Second Reader

Approved: ___*Adam Miller, Ph.D.*_____
Biology Honors Faculty Representative

Approved: _____*Chris Sinclair, Ph.D.*_____
Clark Honors College Representative

Animal behaviors result from complex network activity in the brain. Precise excitation and inhibition within these networks are partially regulated by neuromodulatory systems that regulate the behavior of other neurons, influencing brain processing and ultimately the animal's behavior. This regulation is accomplished, in part, by the neuromodulators acetylcholine (ACh) and noradrenaline (NA). ACh and NA are produced and released by cholinergic and noradrenergic neurons, respectively, and have broad functions throughout the central nervous system. This project investigates the relationship between ACh and NA neuromodulatory activity and

behavioral state with respect to arousal and behavior-dependent modes of neuromodulation. Using systems neuroscience techniques, such as intracranial viral injections and two-photon microscopy, this project offers novel insights into the dynamic relationship between ACh and NA activity and behavioral state in mice. First, I confirm previous findings of a strong relationship between neuromodulatory activity and arousal state, as measured by walking velocity, whisking, and pupil dilation/constriction. Second, I demonstrate that increases in both ACh and NA axonal activity closely track and precede the onset whisking bouts, but not walking. Last, I show that ACh axonal activity across the cortex is significantly less correlated during whisking and walking compared to stationary periods. This project furthers our current knowledge of the relationship between neuromodulatory activity and observable patterns of behavior by offering new evidence of more localized, state-dependent modes of neuromodulation.

Acknowledgements

I would first like to thank Dr. David McCormick and Dr. Lindsay Collins for your incredible mentorship during my time in lab. I have gathered an innumerable amount of knowledge and skills while completing this multi-year project. I will undoubtedly miss our formal data collection and writing check-ins, journal club meetings, and casual chats in the hallways of Huestis hall. These last few years have allowed me to further my passion of learning more about the beautiful, yet mysterious mammalian brain.

I would also like to thank the other current and former members of the McCormick lab. Your expert advice and helpful troubleshooting tips were invaluable as I completed my project. Thank you for creating such a friendly, supportive, and creative environment to complete my thesis.

Thank you to Lanch McCormick, Dr. Roger Thompson, Dr. Nathan Tublitz, and Jenni Van Wyk for your supportive mentorship and advising during my undergraduate career and preparation for medical school. Starting medical school at Case Western Reserve University School of Medicine this upcoming July, I go forward with confidence and preparation to face any challenges that I may encounter.

The completion of this thesis process and my undergraduate coursework in Biology would not be possible without the continued support of the Clark Honors College faculty and staff and the Biology Department advising team. Miriam Alexis Jordan, thank you for making the thesis writing and submission process as seamless as possible. Ingrid Newman and the Biology advising staff, thank you for your endless

help while planning my four years at the University of Oregon and ensuring that I completed all degree and premedical requirements in a timely and efficient manner.

Last, I would be remiss if I did not thank my family for their unwavering and unconditional love and support during my undergraduate career. I am humbled by your endless sacrifices and investments made to ensure my personal well-being and that I am able to gain an excellent education. You are all my rock upon which I'm built. I am forever thankful for shaping me into the individual I am today. And, of course, I will always "do my better best."

Table of Contents

List of Figures

Introduction

An animal's ability to engage with a particular task is highly variable. Most individuals who have sat in a long lecture or completed a lengthy homework assignment understand that our ability to gather and process information fluctuates greatly from moment-to-moment. That is, sometimes we are very focused, while other times we are quite disengaged and distracted. However, previous literature demonstrates that there exists an optimal "arousal" state under which an organism can perform at its best (McGinley et al., 2015). Arousal encompasses both brain state, which describes the physiological activity of the brain, and behavioral state, which describes observable behavioral patterns and movements of an organism. Moment-to-moment fluctuations in brain state and arousal can ultimately influence an animal's ability to successfully perform various perceptual or cognitive tasks. Yerkes and Dodson first predicted this relationship in 1908. Shown below, we see that as arousal increases from low to intermediate levels, performance generally increases; however, further increases in arousal from intermediate to high levels generally degrade that performance (Figure 1).

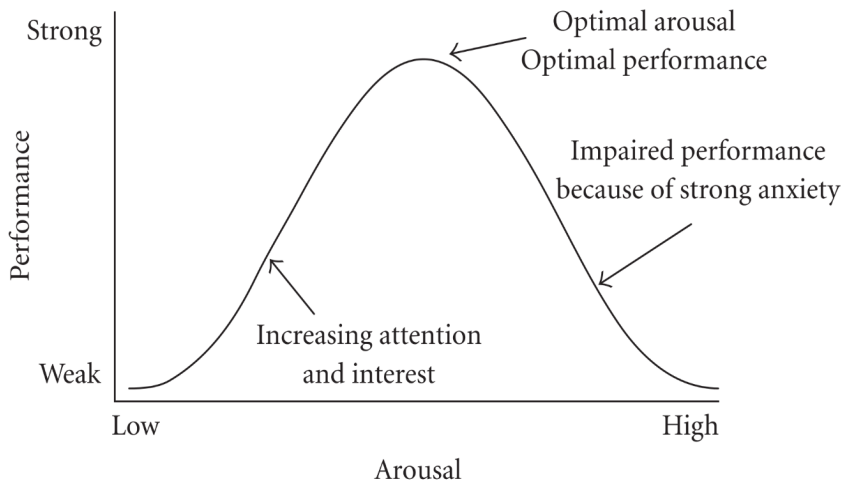

Figure 1. Yerkes and Dodson Law

The Yerkes and Dodson Law states that increases in arousal from low to intermediate levels increase performance, while further increases in arousal from intermediate to high levels degrade that performance. Therefore, there is an optimal level of arousal that results in strongest performance. Figure from Wu et al., 2010.

It is possible to investigate the relationship between changes in arousal-linked behavior and their underlying neural circuitry through a careful analysis of behavioral motifs alongside neural activity. By simultaneously recording external behavioral variables, such as pupil diameter, whisker pad motion, and walking velocity, alongside neural activity within the brain, we are given an overall idea of how changes in behavior are related to changes in neural circuitry. Figure 2 depicts a common behavioral assay through which we can acquire behavioral data while simultaneously recording changes in neural activity (McGinley et al., 2015). While the below behavioral assay provides an overall schematic of what our behavioral recording rigs look like, there are slight differences between the illustration shown here and how this project will evaluate these changes in neural activity. The left of the figure depicts a head-fixed, stationary mouse

performing a behavioral task. As indicated by the colored circles and boxes on the face of the mouse, we can record changes in behavior within these regions using custom computer software. The right of the figure illustrates the entirety of this behavioral set-up. A stationary, head-fixed mouse is free to run on a cylindrical wheel. While recording neural activity, via electrophysiology or microscopy, we can simultaneously record various behavioral motifs reflected on the face of the mouse, as previously described, in addition to walking velocity that is recorded using a rotary encoder in the cylindrical wheel.

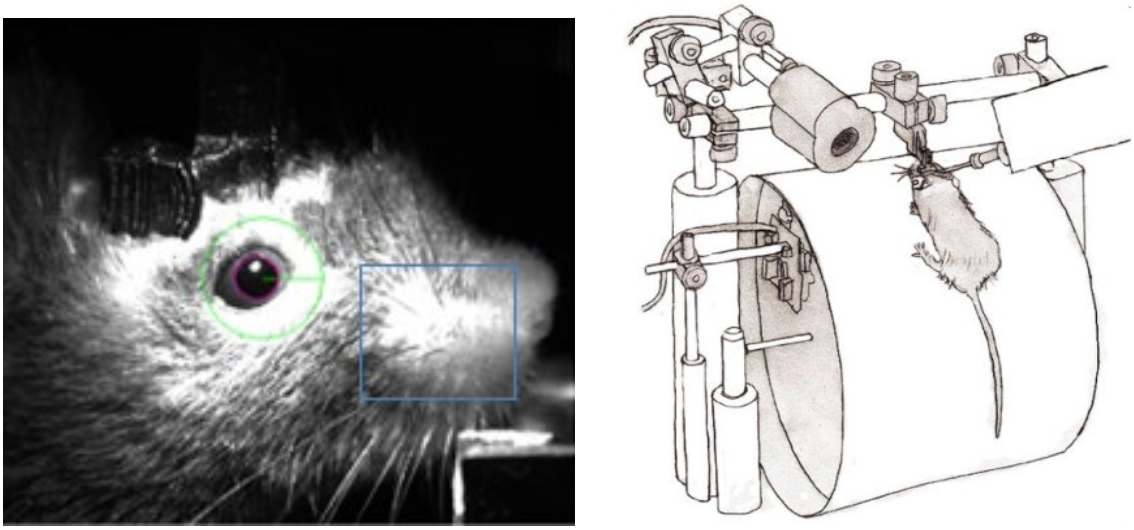

Figure 2. Sample Behavioral and Neural Activity Recording Set-Up

This behavioral assay allows for behavioral data acquisition, including: pupil diameter, whisker motion, snout motion, grooming behaviors, and walking velocity. We can simultaneously record behavior and activity within the brain to identify relationships between changes in neural circuitry and external, observable pattern of behaviors. Figure adapted from McGinley et al., 2015.

A basic understanding of the structure and function of neural cells within the brain is necessary to better understand how these experimental methods allow us to directly visualize real-time changes in neural activity. A neuron is a nerve cell located within the brain or spinal cord that communicates with other neurons to ultimately control various aspects of how the brain functions. The soma, or cell body, of a neuron is the central body of the cell wherein the nucleus is housed and most biochemical processes occur. Extending from the soma are axons and dendrites. Axons are projections from the soma through which electrical signals propagate and generally result in some form of extracellular chemical release from axon terminals. These chemicals then bind to a different neuron's dendrites, which receive the signal and cause biochemical changes within the cell itself. Seen below is the basic structure of a neuron (Figure 3).

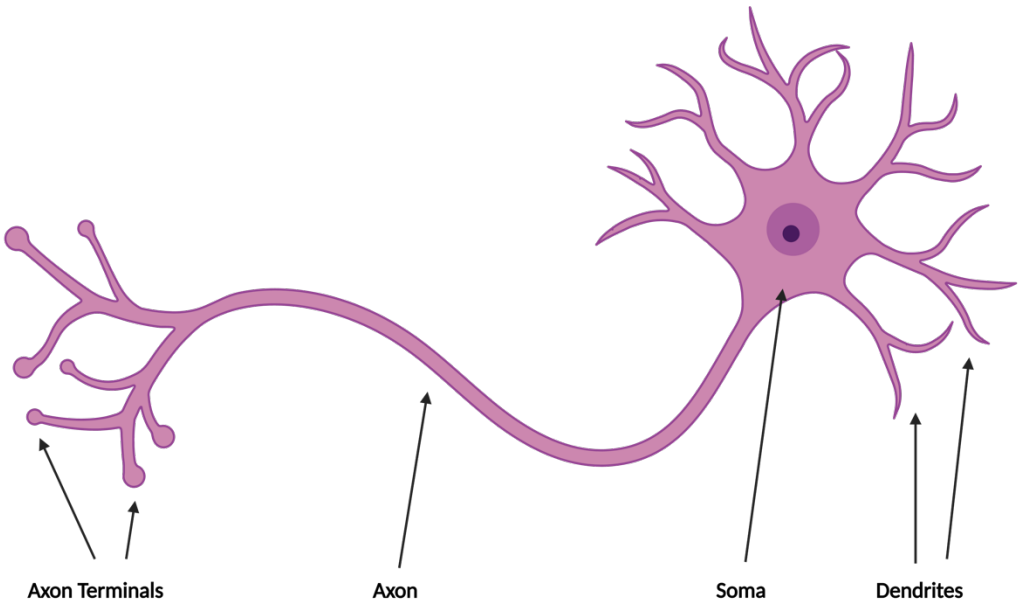

Figure 3. Basic Neuronal Structure

Electrical signals are propagated through the axon and generally result in chemical release from axon terminals. These chemical signals then bind to the dendrites of a receiving neuron, thereby causing biochemical changes within the soma, or cell body, of the cell.

When at rest, the cell body of a neuron is negatively charged compared to its extracellular environment. This difference in charge between the intracellular and extracellular environments is known as the membrane potential. The resting membrane potential of a typical neuron that is not firing or communicating with other neurons is approximately -70 millivolts (mV). When the membrane potential of a neuron reaches a certain threshold value, around -50 mV, a series of ion channels, which allow for the transfer of ions such as sodium or calcium into and out of the cell, activate in such a way that there is a rapid and very large positive change in the membrane potential. This process is known as depolarization. A depolarization to around +30 mV results in the release of neurotransmitters, the technical term for secreted chemical signals from axon terminals. Neurotransmitters are secreted into the synaptic cleft, a 20-40 nanometer (nm) space between the axons and dendrites of neighboring neurons. It is this process of firing an action potential, the more technical term describing this rapid depolarization, that results in neurotransmitter release. As described previously, released neurotransmitter binds to the dendrites of neighboring target neurons and causes downstream effects.

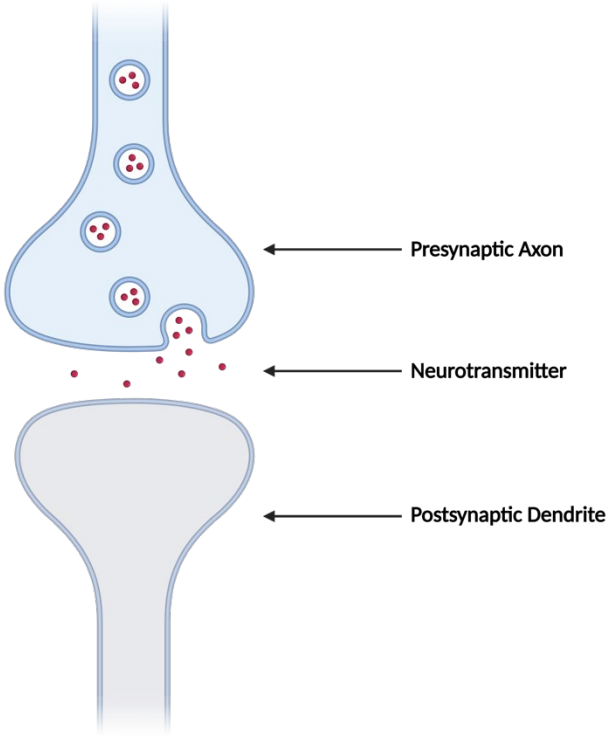

Figure 4. Diagram of Example Synapse

Neurotransmitter is released from the presynaptic axon into the synaptic cleft and binds to the postsynaptic dendrite.

Neuroscientists can directly measure the changes in membrane potential of neurons throughout various regions of the brain to identify when these neurons are active. There are many ways to record these changes in membrane potential, such as electrophysiology and calcium imaging. Electrophysiology, as depicted in Figure 2, directly measures differences in charge between the intracellular and extracellular environments of the neuron. Calcium imaging, which is the method through which I will record neuronal activity, uses indicators that fluoresce in the presence of calcium,

which is involved when the membrane potential reaches threshold and fires an action potential.

Previous literature indicates that external, observable changes in behavior, such as pupil dilation/constriction and walking, are closely related to membrane potential changes in auditory cortical neurons of awake mice (McGinley et al., 2015). Figure 3 shows that pupil dilation/constriction and walking are both closely related to changes in the membrane potential of auditory cortical neurons. In other words, as neurons within the auditory cortex of a mouse become more active, we also observe increases in walking velocity and pupil diameter. Given these data, we can therefore utilize external, observable behavioral motifs as accurate and reliable metrics to partially explain these moment-to-moment fluctuations in behavioral and arousal state and their underlying neural circuitry.

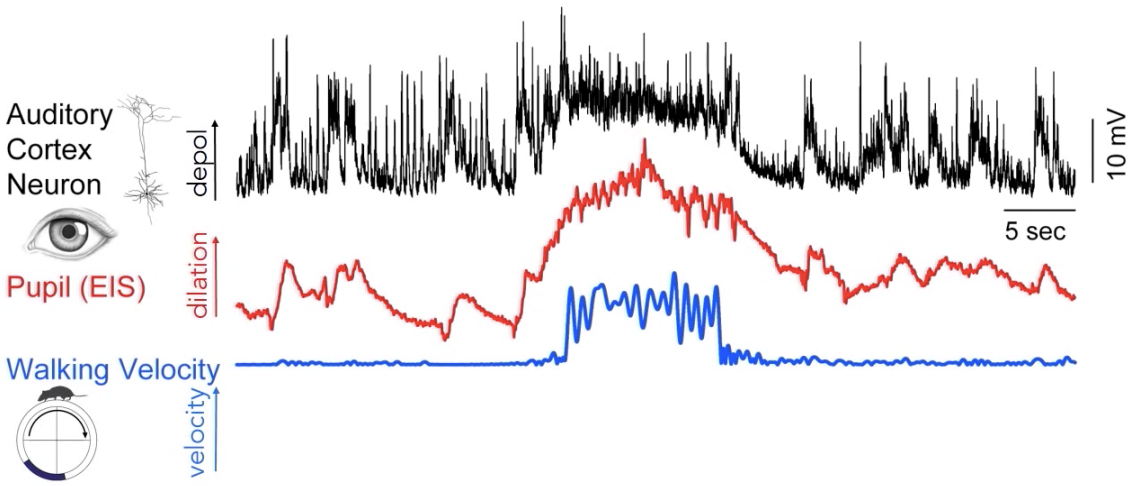

Figure 5. Auditory Cortical Neuron Firing Alongside Changes in Pupil Diameter and Walking

Depolarization of the membrane potentials of auditory cortical neurons are closely related to increases in pupil diameter dilation and increases in walking velocity. As both walking velocity (bottom trace) and pupil diameter (middle trace) begin to increase, we see a simultaneous depolarization in auditory cortical neurons (top trace). The membrane potential of the auditory cortical neurons remains depolarized during the entirety of the pupil dilation and walking velocity events. Figure from McGinley et al., 2015.

As described previously, neurons communicate with one another through the production, release, and binding of neurotransmitters. Rapid variation in behavioral state is, in part, influenced by various neuromodulatory systems within the brain (Figure 6; McCormick et al., 2020, Totah et al., 2018, McGinley et al., 2015, and Picciotto et al., 2012).

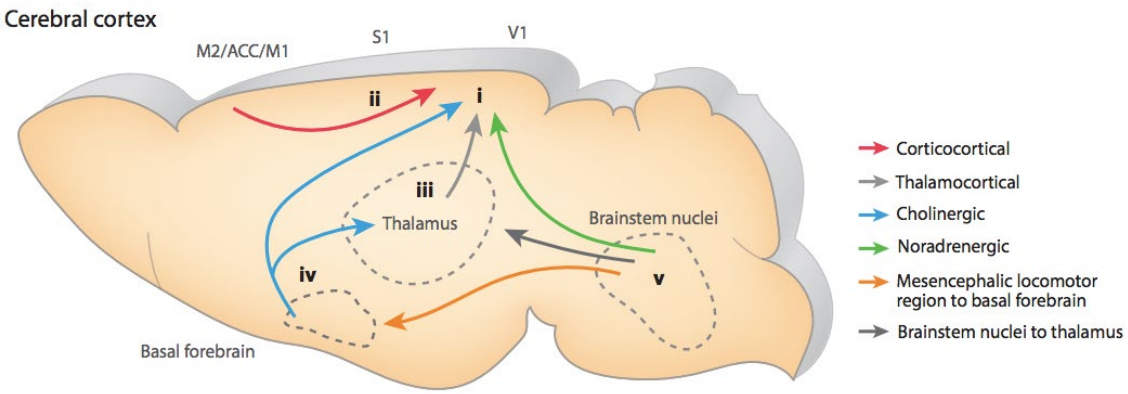

Figure 6. Schematic of Neuromodulatory Circuitry in the Mouse Brain

Various cognitive processes are influenced by neuromodulatory systems that project to various target regions within the brain. Additionally, various brain regions are also influenced by cortical feedback and subcortical inputs. Figure from McCormick et al., 2020.

Neuromodulators are neurons that modulate the activity of other neurons through the production and release of excitatory or inhibitory neurotransmitters. Two predominant neuromodulatory cell types of interest to systems neuroscientists are cholinergic and noradrenergic neurons. Cholinergic neurons produce and release the neurotransmitter acetylcholine (ACh), and noradrenergic neurons produce and release the neurotransmitter noradrenaline (NA). Cholinergic projections from nuclei in the basal forebrain (BF) and noradrenergic projections from nuclei in the locus coeruleus (LC) innervate various target regions in the cortex, ultimately influencing cognition and sensory processing (Figure 7; McCormick et al., 2020).

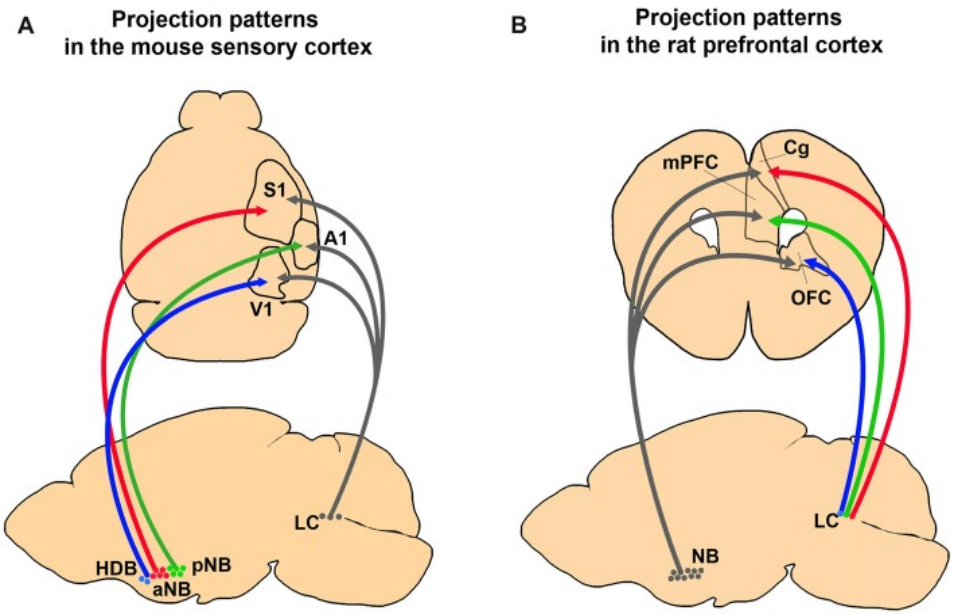

Figure 7. Cortical Projections from the Basal Forebrain and Locus Coeruleus

Cholinergic projections from nuclei in the basal forebrain and noradrenergic projections from nuclei in the locus coeruleus innervate target regions within the cortex. Activity within these nuclei modulate various regions of the cortex, thereby influencing sensory processing and behavior. Left: S1: primary somatosensory cortex; A1: primary auditory cortex; V1: primary visual cortex; LC: locus coeruleus; HDB: horizontal diagonal band nucleus; aNB: anterior nucleus basalis; pNB: posterior nucleus basalis. Right: Cg: cingulate gyrus; OFC: orbitofrontal cortex; mPFC: medial prefrontal cortex; NB: nucleus basalis; LC: locus coeruleus. Figure taken from Rho et al., 2018.

Interestingly, changes within cholinergic and noradrenergic neuromodulatory activity have also been found to be closely linked to changes in behavioral state and arousal state (Reimer et al., 2016). Figure 8 shows this relationship between neuromodulatory activity and changes in pupil diameter. Increases in both acetylcholine and noradrenaline precede pupil dilation. These data, coupled with evidence that pupil diameter is a reliable and accurate external metric of arousal state (Gielow et al., 2017, Joshi et al., 2016, and McGinley et al., 2015), suggests that changes in neuromodulatory activity are closely linked to changes in arousal state. This project aims to deepen our current knowledge of the relationship between changes in neuromodulatory activity and observable patterns of behavior in mice.

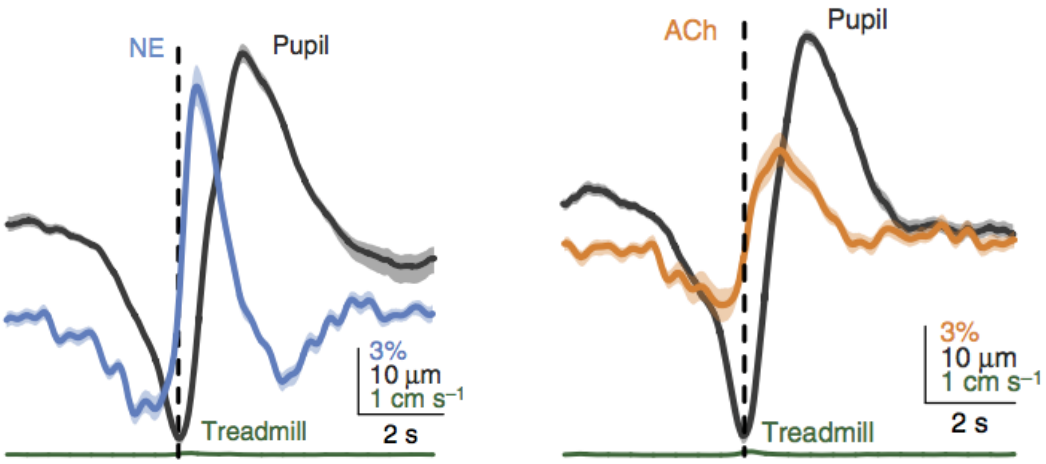

Figure 8. Noradrenergic and Cholinergic Neuromodulatory Activity and Changes in Pupil Diameter

The blue trace (left) represents noradrenergic axon activity, and the orange trace (right) represents cholinergic axon activity relative to the onset of an increase in pupil diameter (dashed line). While this figure uses the term norepinephrine (NE), these data still demonstrate changes in noradrenergic neuromodulatory activity since noradrenaline is also called norepinephrine. The black trace represents pupil diameter. Increases in both noradrenergic and cholinergic axon activity precede the onset of pupil dilation. Figure from Reimer et al., 2016.

It was previously thought that neuromodulatory systems within the central nervous system behave in a global, synchronous manner (Lee et al., 2012). However, recent studies have offered new insights into more regionally-specific, state-dependent modes of neuromodulation (Laszlovszky et al., 2020, Chandler et al., 2019, Obermayer et al., 2017, and Zagha et al., 2014). This project investigates the relationship between cholinergic and noradrenergic neuromodulatory activity and behavioral state with respect to diverse arousal and behavior-dependent modes of neuromodulation. That is, this study elucidates how neuromodulation is related to observable behavior as an

animal's arousal and behavioral state changes over time. My project investigates this relationship between neuromodulation and behavior in three ways. First, I confirm the relationship between neuromodulatory activity and arousal state, with respect to the specific behavioral motifs of walking, whisking, and pupil dilation/constriction. Second, I determine the temporal relationship between changes in neuromodulatory activity and both the onset and offset of these behavioral events. Third, I determine whether ACh and NA neuromodulation is specific to particular regions within the brain or if there is widespread synchrony of neuromodulatory systems across the brain during fluctuating arousal states. I predict that data obtained from my project will demonstrate that ACh and NA activity is more correlated with behavioral measures of arousal than would be predicted by chance, ACh and NA activity precedes behavioral changes more than would be predicted by chance, and that there exists widespread synchrony of these neuromodulatory systems across the brain during fluctuating arousal states.

Methods

Animals

A mouse model organism offers powerful genetic tools that have been developed to study neural processes. In this study, a total of 5 (N = 5) transgenic mice were used to investigate the relationship between neural circuitry and behavior. A cohort of 2 (n = 2) ChAT-cre strain mice and a cohort of 3 (n = 3) DBH-cre x Ai162 strain mice were used in experimental trials and during data analysis. In this study, ChAT-cre mice will be abbreviated to ChAT, and DBH-cre x Ai162 mice will be abbreviated to DBH. Following surgical procedures and during experimentation, mice were singly housed and were given access to food and water ad libitum. All experimental procedures utilizing live mice were approved by the University of Oregon Institutional Animal Care and Use Committee. This protocol was also in compliance with the National Institutes of Health Guide for the Care and Use of Laboratory Animals.

Rodent Surgeries

To visualize cholinergic cortical activity in awake mice, we used viral administration of a fluorescent calcium indicator, GCaMP6s. GCaMP6s is a genetically-encoded fluorescent calcium indicator used to track neuronal activity. When injected into the basal forebrain of ChAT mice, GCaMP6s is expressed only in cholinergic cells. Viral replication throughout the cell allows for GCaMP6s expression in far-reaching axons and dendrites. DBH mice transgenically express a cre-dependent form of

GCaMP6s. Therefore, viral administration of GCaMP6s into the locus coeruleus was not required for noradrenergic cortical activity visualization.

To conduct stereotactic intracranial viral injections in ChAT mice, animals were first anesthetized with 4% isofluorane and were continually sedated via consistent 1.2% oxygen and 2% isofluorane inhalation. Once sedated, mice were injected subcutaneously with Meloxicam SR (6 mg/kg) to mitigate pain following the surgical procedure. After the surgical area at the top of the scalp was shaved to remove fur and sterilized using betadine and isopropyl alcohol, a posterior to anterior medial incision was made to expose the surface of the skull. At this time, the scalp and fascia were scraped away such that visualization of the skull was unobstructed. The mouse's head was then positioned such that the anterior and posterior sides of the skull were level along the Z-plane. A mark was placed 1.44 mm laterally and 0.6 mm posteriorly to bregma, a landmark suture of the skull indicating the intersection of the frontal and parietal bones of the skull.

Using a dental drill, a craniotomy approximately 1 mm in diameter was made so that the surface of the brain was visible. A glass micropipette containing the axon-targeted GCaMP6s viral solution was then slowly lowered to 3.8 mm below the surface of the brain (Figure 9). A total of 1000 nanoliters (nL) of GCaMP6 virus was injected into basal forebrain in these ChAT mice over the timespan of approximately 10 minutes. The pipette remained within the brain for an additional 15 minutes to allow for sufficient viral diffusion. Following this diffusion period, the pipette was slowly removed, the scalp was folded back over the skull, and the incision was closed using

Vetbond adhesive. Mice remained in a temperature-controlled recovery chamber for 3 days following the surgery and were monitored daily to ensure proper recovery.

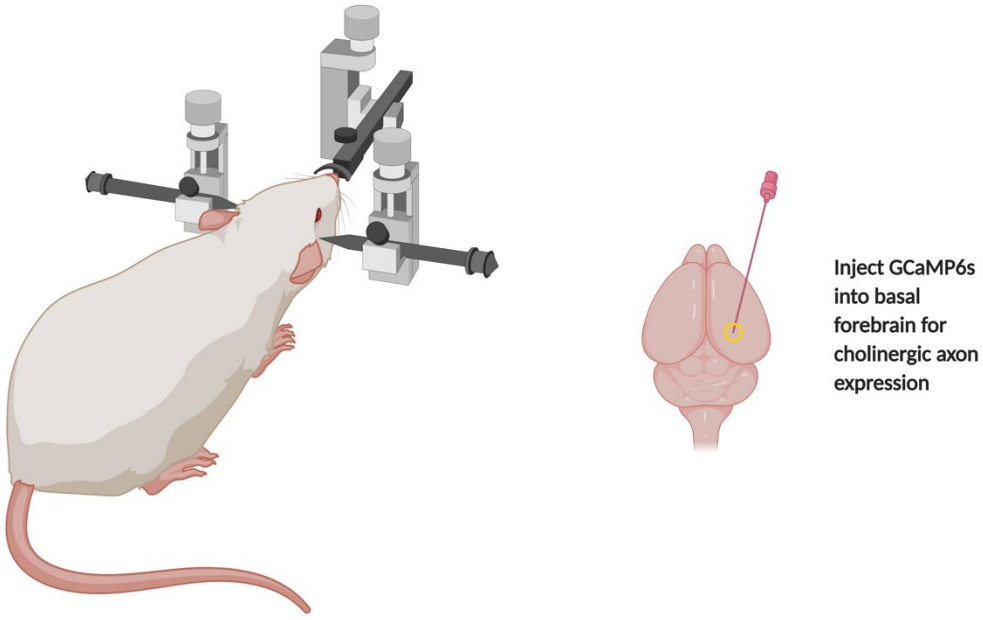

Figure 9. Example Stereotactic Viral Injection of a ChAT Mouse

ChAT mice were stereotactically injected with GCaMP6s virus into the basal forebrain. Introduction of this fluorescent calcium indicator allows for a visualization of cholinergic axon activity. Injection of GCaMP6s into the locus coeruleus of DBH mice was not necessary for visualization of noradrenergic axon activity.

Approximately 14 days following the completion of the viral injection in ChAT mice, both ChAT and DBH mice were implanted with a surgical headpost along the surface of the skull. This time period was chosen based on preliminary evidence that GCaMP6s expression is observed in the cortex 2 weeks post-injection. The headpost

allows mice to remain stably head-fixed within our experimental recording rig. Along with implantation of the headpost, an 8 mm glass cranial window was installed to allow for direct visualization of the surface of the brain.

Two-Photon Axon Imaging

Simultaneous two-photon axon imaging and behavioral data acquisition allows us to directly compare axonal activity to behavioral state. Using a ThorLabs two-photon mesoscope (Sofroniew et al., 2016), we simultaneously measured real-time axonal fluorescence from multiple cortical regions. While recording axonal fluorescence data at approximately 10 Hz from multiple regions of interest (ROIs) across the cortex, real-time pupil constriction/dilation recordings, walking velocity, and whisking behaviors were also acquired, as described below. A cohort of 2 ChAT mice were recorded and analyzed and included a total of 6 recording sessions of 184 axons across 27 ROIs. A cohort of 3 DBH mice were recorded and analyzed and included a total of 7 recording sessions of 94 axons across 24 ROIs.

Behavioral Data Acquisition

Using a separate camera placed to the side of the mouse's face, we collected other metrics of behavioral state, including pupil diameter and whisker pad motion energy (Figure 10). Angular walk velocity was measured via a rotary encoder attached to the cylindrical walking wheel. Changes in walk velocity are considered a bout of walking when the angular walk velocity exceeds 2.5 cm/s for greater than 1 second and is preceded and followed by 2 seconds of stillness. Whisker pad motion energy is defined as the total change in pixel intensity from one frame to the next across an

approximately 1 mm square region over the whisker pad. Motion energy was then normalized between 0 and 1. A whisking bout is defined as when whisker motion energy exceeds 20% of the normalized whisking trace. This whisk must also last longer than 1 second and must be preceded and followed by 2 seconds of stillness. Changes in pupil size are represented as a percent change of maximum pupil diameter across the recording session.

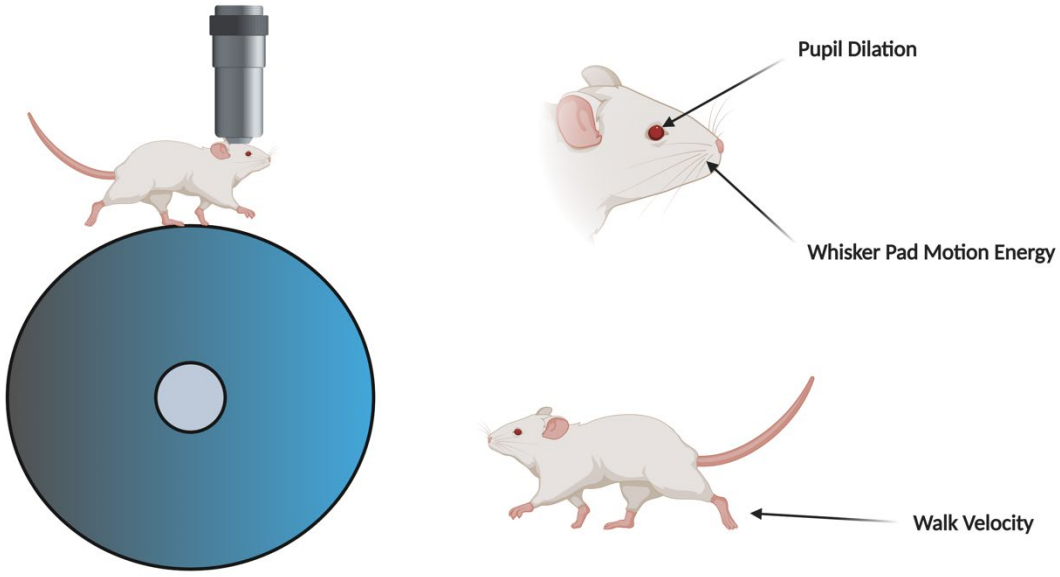

Figure 10. Simultaneous Two-Photon Calcium Imaging and Behavioral Data Acquisition

Simultaneous two-photon axon imaging (left) and behavioral data acquisition (right) allows for a direct comparison of changes in neuronal fluorescent activity and changes in behavioral state.

Histology

To confirm that we were actually recording from either cholinergic or noradrenergic axons, histological verification of the neuromodulatory nuclei was performed. Once experiments were complete, animals were sacrificed using a CO2 chamber. Mice were then intracardially perfused with approximately 20-50 milliliter (mL) 0.01 molar (M) phosphate buffer saline solution (PBS) followed by 4% paraformaldehyde in phosphate buffer to stably fix the brain for further examination. Whole, intact brains were post-fixed in 4% paraformaldehyde for 24 hours to allow for further fixation. Brains were then sectioned into 50-60 micron (μm) coronal sections and immunostained for green fluorescent protein. This immunostaining was performed by rinsing the tissue in PBS, permeabilizing the cell membranes with 0.03% Triton, blocking in Normal Donkey Solution, and incubating in primary antibody solution overnight. During the following day, tissues were rinsed again, incubated in a secondary antibody solution conjugated with a red fluorophore, rinsed again, and mounted on glass slides. Once complete, sections were placed on glass microscope slides and coated with SlowFade Antifade Mountant with DAPI. A class coverslip was also applied. Sections were visualized using a spinning-disk confocal microscope at 10-20x magnification.

Data Analysis

After data acquisition was completed, data was analyzed using custom MATLAB code. Specifically, MATLAB was used to analyze fluorescence data and to quantify relationships between varying signals. A measure of a change in fluorescence over baseline fluorescence, or ΔF/F, was utilized as a primary metric to indicate changes in fluorescent axonal activity. ΔF/F was used in order to provide an accurate

indication of any increases in axonal fluorescence with respect to basal levels of fluorescence. The median fluorescence value for each recording session was used as the baseline fluorescence value. ΔF/F was then calculated using the following equation: $\frac{\Delta F}{F} = \frac{F_t - F_0}{F_0}$, where F_t is the fluorescence at a specified time point, and F_0 is baseline fluorescence.

Custom MATLAB scripts were used for all statistical analyses. The function 'xcorr' was used to calculate cross-correlation between axons and between axon activity and behavior. A Student's t-test (alpha = 0.5) was used to identify any significant differences in max cross correlation between axonal activity and the onset of behavioral events. A one-way ANOVA (alpha = 0.5) was used to identify any significant differences in average max cross correlation between axons during varying behavioral states.

Results

Verification of Green Fluorescent Protein Labeled Cells in the Basal Forebrain and Locus Coeruleus

To determine if my GCaMP6s viral injections were successfully localized to the basal forebrain in ChAT mice and if DBH mice natively expressed GCaMP6s fluorescence, brains of one ChAT mouse and one DBH mouse were immunostained for green fluorescent protein (GFP). Sections through the basal forebrain (ChAT) and locus coeruleus (DBH) were collected and stained such that microscopic visualization of GFP labeled cells in these neuromodulatory nuclei was possible. Below are sample imaging data demonstrating these results. The successful staining and fluorescent visualization of GFP labeled cell bodies in the basal forebrain (left) and locus coeruleus (right) demonstrate that my viral injections into the basal forebrain of ChAT mice were successful and that DBH mice do indeed express GCaMP6s fluorescence (Figure 11). These images were acquired using a spinning disk confocal at 10-20x magnification, and slides were imaged less than 1 week following immunostaining protocol. Since fluorescence was localized to these neuromodulatory nuclei, and since a high proportion of cholinergic and noradrenergic cell bodies are localized to these respective nuclei, these histological findings confirm that subsequent axonal fluorescent imaging accurately reflects changes in either cholinergic or noradrenergic neuromodulatory activity.

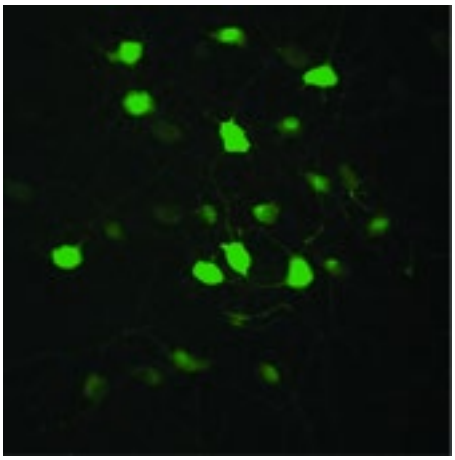

GFP Labeled Cell Bodies in the Basal Forebrain

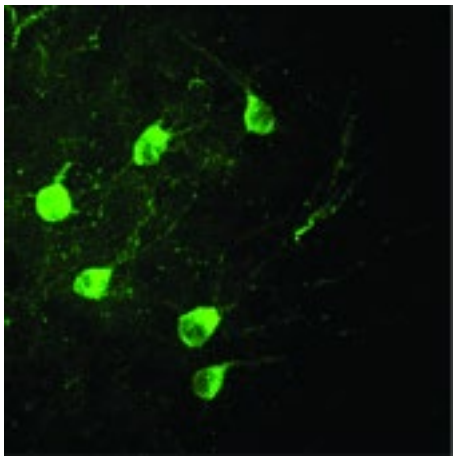

GFP Labeled Cell Bodies in the Locus Coeruleus

Figure 11. GFP Labeled Cell Bodies in the Basal Forebrain and Locus Coeruleus

Histological staining and imaging show fluorescently labeled cell bodies in the basal forebrain (left) and locus coeruleus (right).

Confirmation of the Relationship Between Neuromodulation and Behavioral State

The first aim of this project was to confirm previously reported relationships between neuromodulatory activity and behavioral state with respect to specific behavioral motifs, such as pupil dilation/constriction, walking, and whisking (McCormick et al., 2020 and Reimer et al., 2016). To accomplish this goal, two-photon calcium imaging was conducted to simultaneously acquire neuromodulatory axonal fluorescence in the cortex of awake mice and external behavioral markers of changing brain and arousal states. Below depicts a single experimental recording session where a head-fixed mouse was free to run on a wheel while two-photon calcium imaging and behavioral data collection was conducted (Figure 12). As shown on the right, changes in

pupil size and facial movements were recorded in real-time alongside changes in axonal fluorescence, as shown on the left. Performing two-photon microscopy while simultaneously recording behavioral motifs using a camera directed at the mouse's face allows for the accurate acquisition of changes in neuromodulatory-related axonal fluorescence as the behavioral state of the mouse fluctuates from moment-to-moment. For example, as the animal's pupil diameter or whisker pad motion energy increases (right), we simultaneously observe notable changes in axonal fluorescence (left).

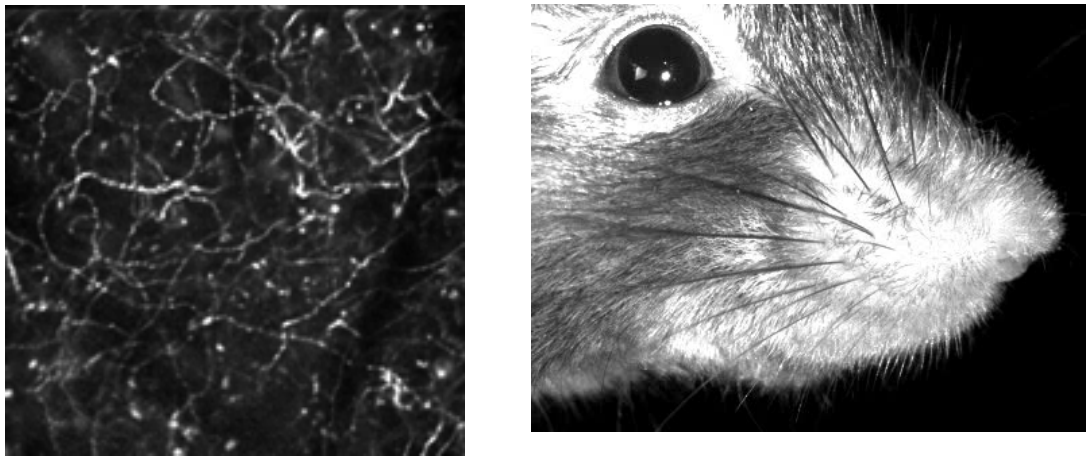

Figure 12. Simultaneous Two-Photon Axon Imaging and Behavioral Data Acquisition

Left: Calcium-dependent fluorescence from axons in the cortex of an awake mouse. Right: Example image of a face recording from which pupil diameter and whisker motion energy were captured.

To demonstrate these changes in axon activity in relation to moment-to-moment fluctuations in behavioral and arousal state, I measured the fluorescence of localized groups of cortical axons (ROIs) and compared their behavior in relation to external metrics of changing behavioral state. In the below figure, raw traces of pupil diameter,

whisker motion energy, and walking velocity are temporally aligned to GCaMP6s activity in cholinergic axons in the cortex of an awake ChAT mouse (Figure 13). The change in fluorescence relative to baseline fluorescence, ΔF/F, was recorded from a total of 10 axons from 5 ROIs, with each ROI being represented by differently colored traces. As indicated by the red, dashed boxes, increases in whisker motion energy or walking velocity were both accompanied by increases in standardized pupil diameter and by synchronous increases in axonal ΔF/F across all ROIs. From these data, it is clear that cholinergic neuromodulatory activity increased for the entirety of an animal's walking bout or whisking behavior. Whisking activity alone, with minimal changes in walking velocity, was also associated with increases in ΔF/F (last red, dashed box).

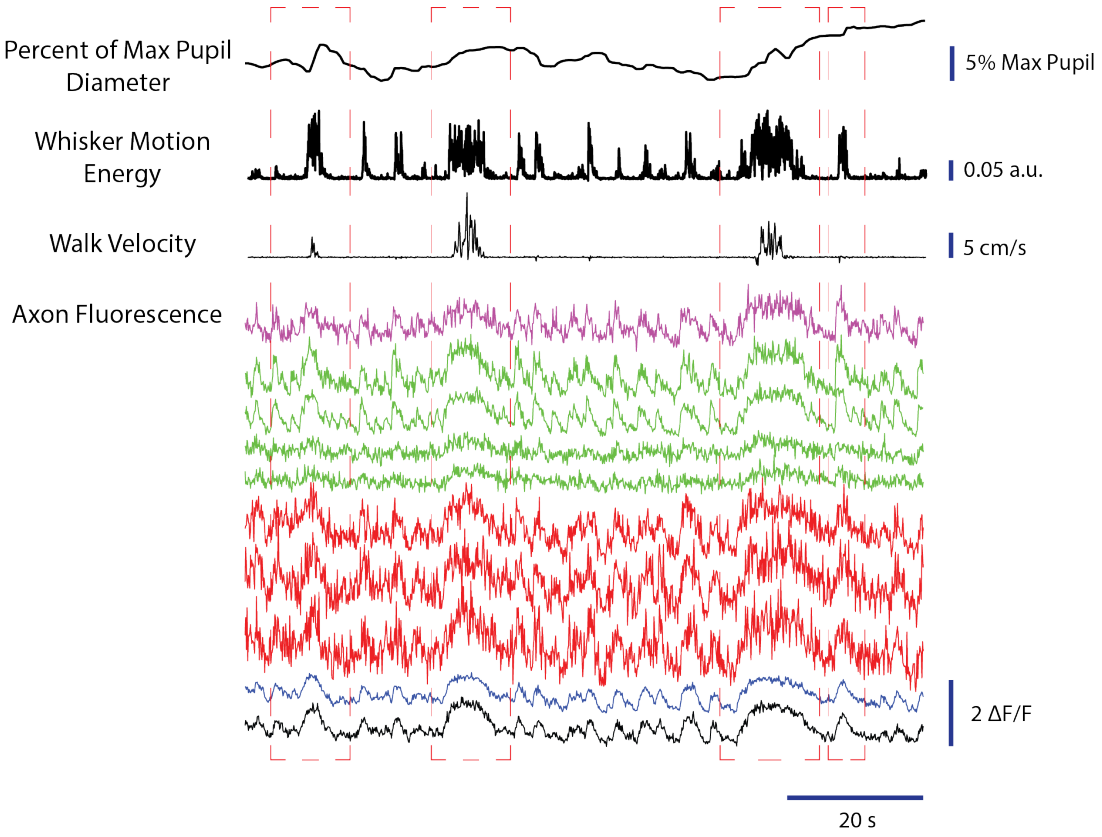

Figure 13. ACh Axonal Fluorescence Compared to Behavioral Measures of Arousal

As an animal whisked and walked, the ΔF/F of cortical axons and pupil diameter also increased. Pupil diameter was normalized to maximum pupil diameter of the animal in a particular recording session. Whisker movement was measured in motion energy (a.u. = arbitrary units). Walking velocity was measured in cm/s. Axonal fluorescence was measured in ΔF/F. Red, dashed boxes indicate bouts of whisking or walking that cause widespread increases in axonal ΔF/F.

Similar observations were made when analyzing the traces of noradrenergic cortical axons. Figure 14 shows raw traces of pupil diameter, whisker motion energy, and walking velocity all temporally aligned to noradrenergic axons in the cortex of an awake, DBH mouse. ΔF/F was recorded from a total of 13 axons from 3 ROIs, with each ROI being represented by differently colored traces. As seen in the noradrenergic raw trace recordings, increases in whisker motion energy and walking velocity were both accompanied by increases in pupil diameter and ΔF/F of cortical axons across all ROIs. Noradrenergic increases in ΔF/F were most prevalent at the onset of a whisking or walking bout, as previously described in the literature (Reimer et al., 2016). Similar to findings in cholinergic axons, increases in whisker motion energy also drove increases in ΔF/F across all noradrenergic ROIs with minimal changes in walk velocity, (second red, dashed box), as compared to other periods of walking.

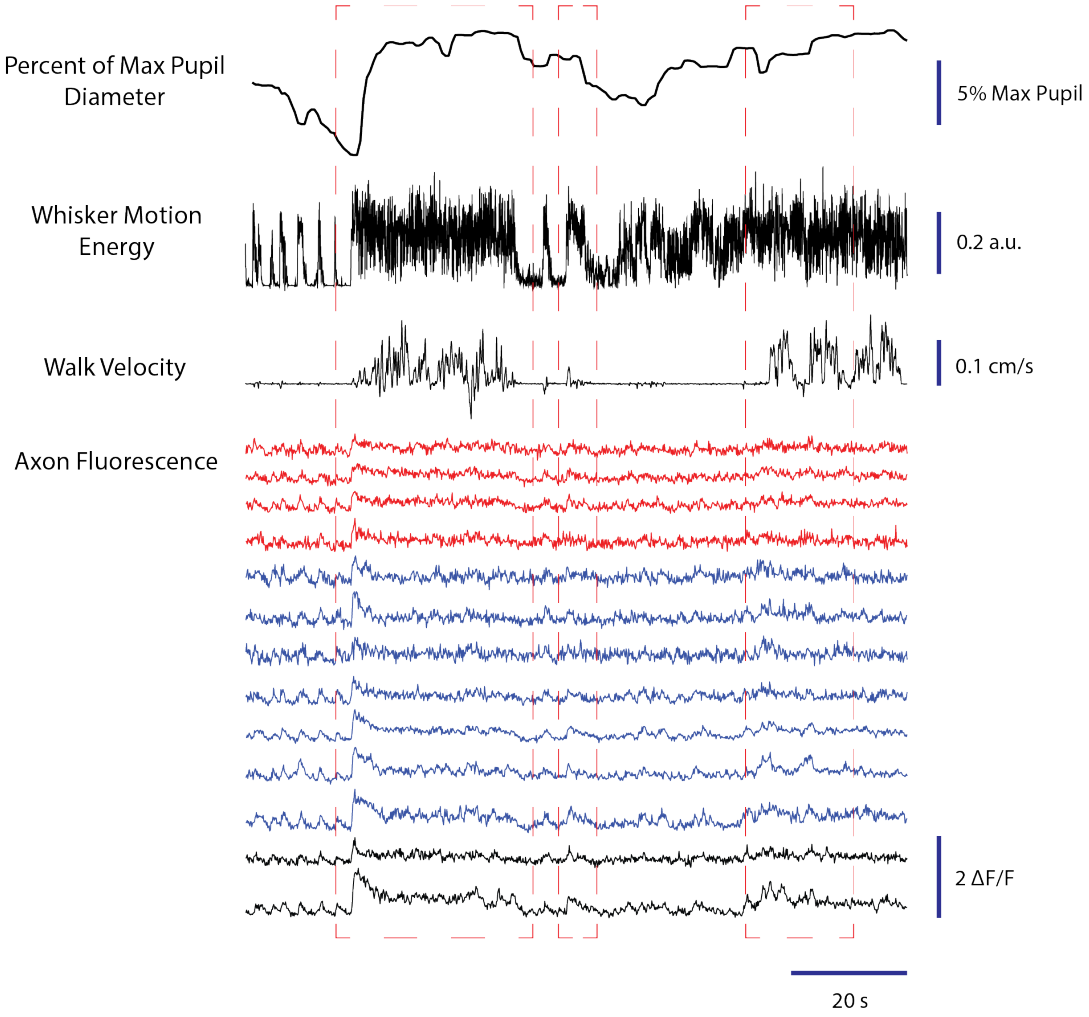

Figure 14. NA Axonal Fluorescence Compared to Behavioral Measures of Arousal

As an animal whisks and walks, the ΔF/F of cortical axons and pupil diameter also increased. Red, dashed boxes indicate bouts of whisking or walking that cause widespread increases in axonal ΔF/F.

Overall, these results demonstrate that both cholinergic and noradrenergic axonal activity closely track changes in behavioral state and arousal. At times of high arousal, mainly during a significant walking or whisking bout, axonal ΔF/F sharply increased. However, at times of low arousal, shown by a lack of walking or whisking and a low pupil diameter, axonal ΔF/F did not significantly increase.

Analysis of the Temporal Relationship between Changes in Neuromodulatory Activity and the Onset and Offset of Behavioral Events

To determine the temporal relationship between ACh and NA neuromodulatory activity and behavioral activity in awake mice, ΔF/F and pupil diameter were collected and aligned to the onset and offset of whisking and walking bouts. Figure 15 shows the results from all ChAT mice recording sessions (n = 6) during the onset of a whisking and walking bout. At the left of the figure, increases in whisker motion energy indicate the onset of a whisking bout (dotted vertical line). Both pupil diameter and ACh axonal ΔF/F increased at the onset of whisking. Interestingly, ACh axon fluorescence tracked increases in whisker motion energy very closely, as compared to pupil diameter, which seemed to slightly lag increases in whisking and took longer for pupillary responses to take effect. At the right of the figure, large increases in walk velocity indicate the onset of a walking bout. Similar to the onset of a whisking bout, both pupil diameter and ACh axonal ΔF/F increased at the onset of walking. ACh axonal fluorescence also increased prior to the onset of a walking bout, sustained high ΔF/F during the duration of the walking bout, and rapidly decreased following the walking event. These data show that ACh axonal activity closely track the onset of whisking bouts, as compared to walking bouts.

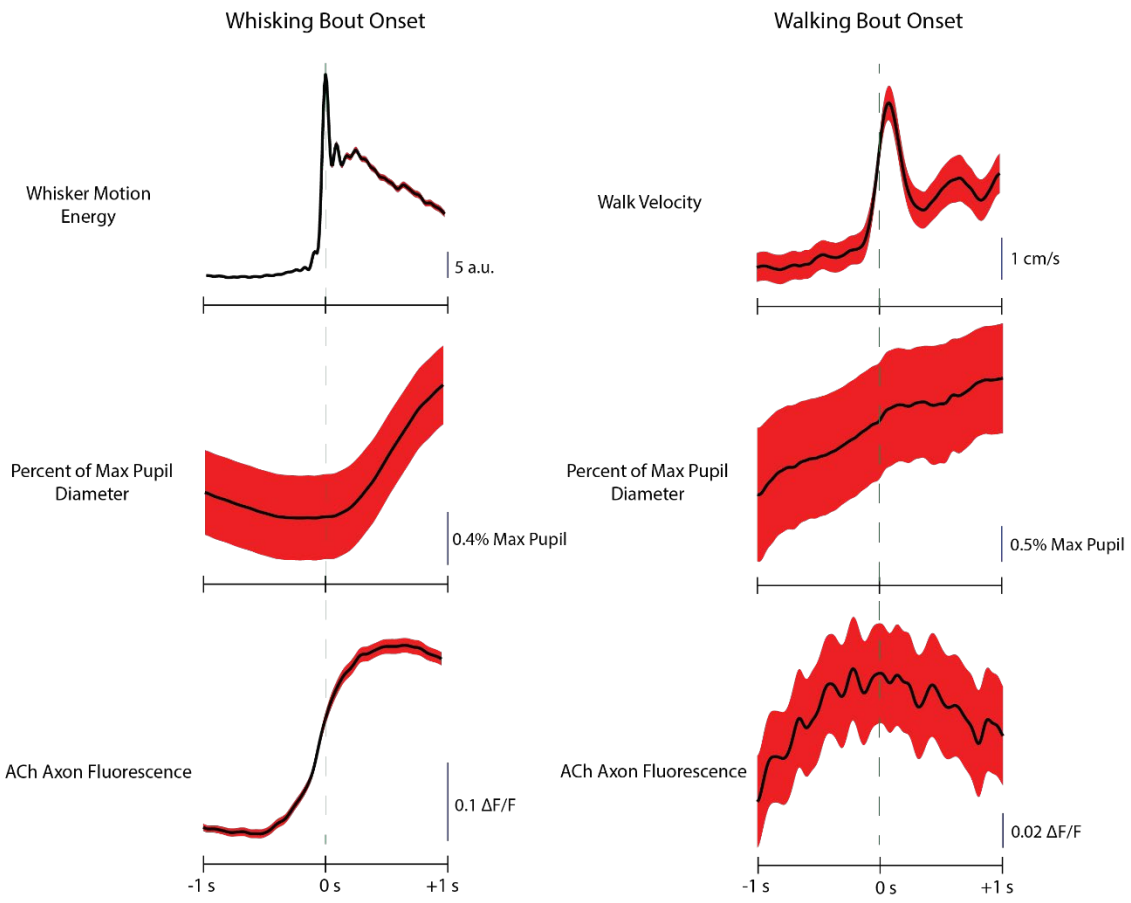

Figure 15. Changes in Pupil Diameter and ACh Axon Fluorescence Temporally Aligned to the Onset of Whisking and Walking Bouts

Increases in whisker motion energy (left) and walk velocity (right) are both plotted alongside increases in pupil diameter (middle) and ACh axonal ΔF/F (bottom). All traces were temporally aligned to 1 second prior and 1 second after the onset of a behavioral event. Data were collected from all ACh mice recording sessions (n = 6). Axonal fluorescence was collected from multiple ROIs across the cortex. Red shading indicates standard error of the mean. The green dashed line indicates timepoint 0 (onset of behavioral event).

Temporally aligning changes in pupil diameter and changes in NA axonal fluorescence yield similar results to that of the cholinergic neuromodulatory system. Figure 16 shows the results from all DBH mice recording sessions (n = 7) during the

onset of a whisking and walking bout. Similar to results from cholinergic axons, increases in whisker motion energy were accompanied by increases in both pupil diameter and NA axonal ΔF/F. We again observed that NA fluorescence closely tracked increases in whisker pad motion energy, but changes in pupil diameter slightly lagged increases in whisking. Walking was also accompanied by increases in pupil diameter and NA axonal ΔF/F. Similar to the cholinergic neuromodulatory system, pupil diameter increased prior to the onset of a walking bout. NA axonal fluorescence also increased prior to the onset of a walking bout, sustained high ΔF/F during the duration of the walking bout, and decreased following the walking event. These data show that NA axonal activity closely track the onset of whisking bouts, but not walking bouts.

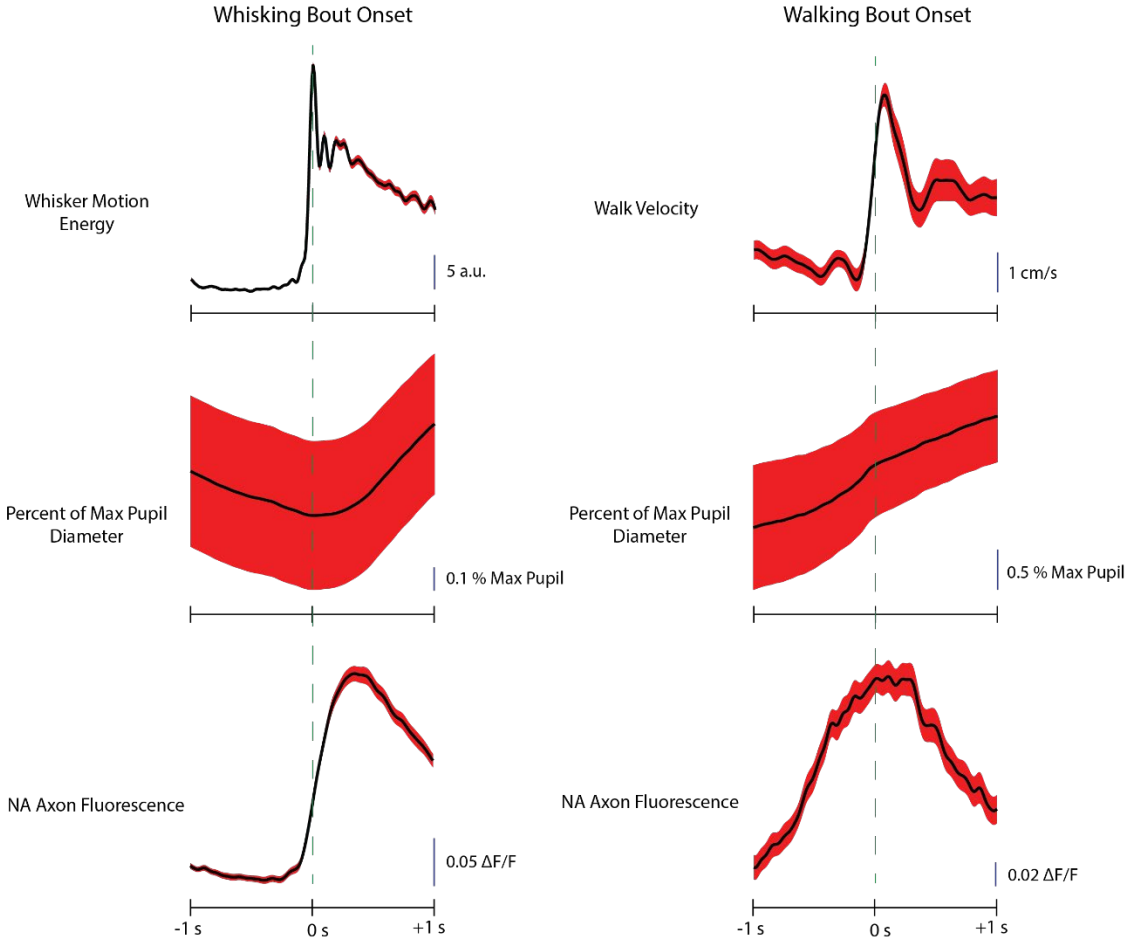

Figure 16. Changes in Pupil Diameter and NA Axon Fluorescence Temporally Aligned to the Onset of Whisking and Walking Bouts

Increases in whisker motion energy (left) and walk velocity (right) are both plotted alongside increases in pupil diameter (middle) and NA axonal ΔF/F (bottom). All traces were temporally aligned to 1 second prior and 1 second after the onset of a behavioral event. Data were collected from all DBH mice recording sessions (n = 7). Axonal fluorescence was collected from multiple ROIs across the cortex. Red shading indicates standard error of the mean. The green dashed line indicates timepoint 0.

Figure 17 depicts ACh axonal activity changes related to the offset of whisking and walking from all ChAT mice recording sessions. At the offset of a whisking bout, both pupil diameter and ACh axon fluorescence generally tracked decreases in whisker motion energy, with a slightly delayed time course. At the offset of a walking bout, however, neither pupil diameter nor ACh axon fluorescence tracked decreases in walking velocity as closely.

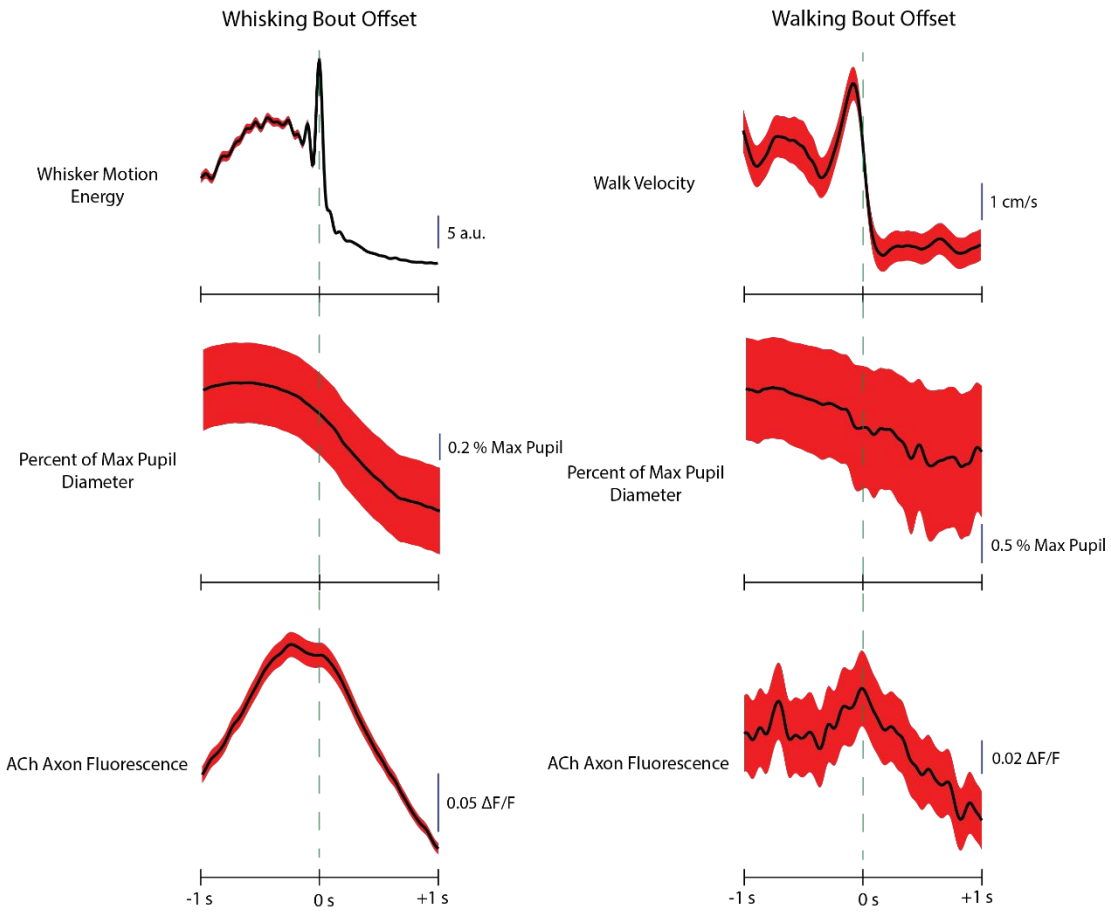

Figure 17. Changes in Pupil Diameter and ACh Axon Fluorescence Temporally Aligned to the Offset of Whisking and Walking Bouts

Decreases in whisker motion energy and walk velocity were both accompanied by decreases in pupil diameter and ACh axonal ΔF/F. All traces were temporally aligned to 1 second prior and 1 second after the onset of a behavioral event. Data were collected from all ChAT mice recording sessions (n = 6). Axonal fluorescence was collected from multiple ROIs across the cortex. Red shading indicates standard error of the mean. The green dashed line indicates timepoint 0.

Temporally aligning changes in pupil diameter and changes in NA axonal fluorescence again yield similar results to that of the cholinergic neuromodulatory system. Figure 18 shows the results from all DBH mice recording sessions aligned to the offset of whisking and walking. Decreases in whisker motion energy were

accompanied by decreases in pupil diameter and NA axonal fluorescence. Both pupil diameter and NA ΔF/F traces decreased and tracked the offset of whisking, with a slightly delayed time course compared to the onset of this behavior. Decreases in walk velocity, indicating the offset of a walking bout, were accompanied by broad decreases in both pupil diameter and NA axon fluorescence.

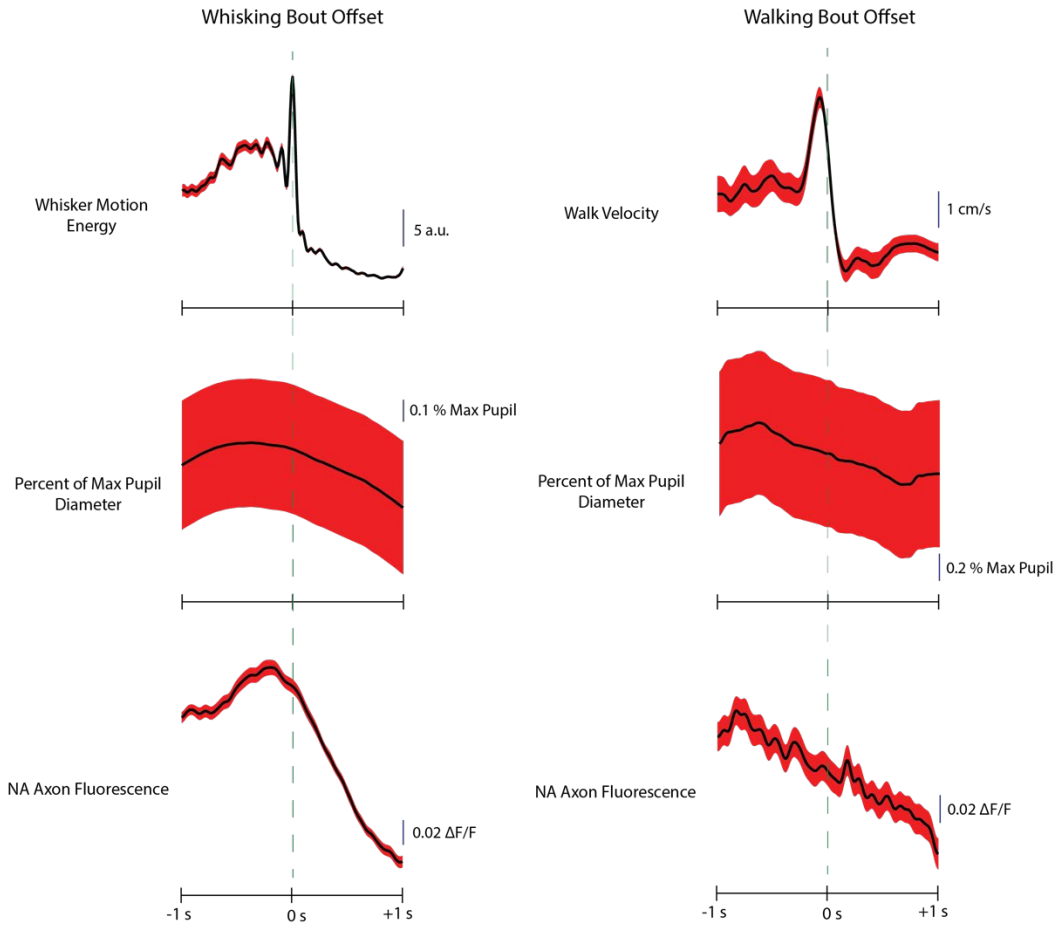

Figure 18. Changes in Pupil Diameter and NA Axon Fluorescence Temporally Aligned to the Offset of Whisking and Walking Bouts

Decreases in whisker motion energy and walk velocity were both accompanied by decreases in pupil diameter and NA axonal ΔF/F. All traces were temporally aligned to 1 second prior and 1 second after the onset of a behavioral event. Data were collected from all DBH mice recording sessions (n = 7). Axonal fluorescence was collected from multiple ROIs across the cortex. Red shading indicates standard error of the mean. The green dashed line indicates timepoint 0.

In order to determine whether axon activity preceded or followed whisking and walking, I calculated cross correlations between either ACh or NA axonal activity and behavior (whisking and walking). Figure 19 shows a representative example of the cross correlation between ACh axonal activity and whisker motion energy and walk velocity in a single ChAT mouse recording session. Peak cross correlation between ACh axonal activity and whisker motion energy peaked prior to timepoint 0, showing that changes in ACh axon activity slightly preceded changes in whisker pad motion energy. Cross correlation between ACh axonal activity and walk velocity peaked after timepoint 0, indicating that ACh neuromodulatory activity preceded whisking behavior, but not walking.

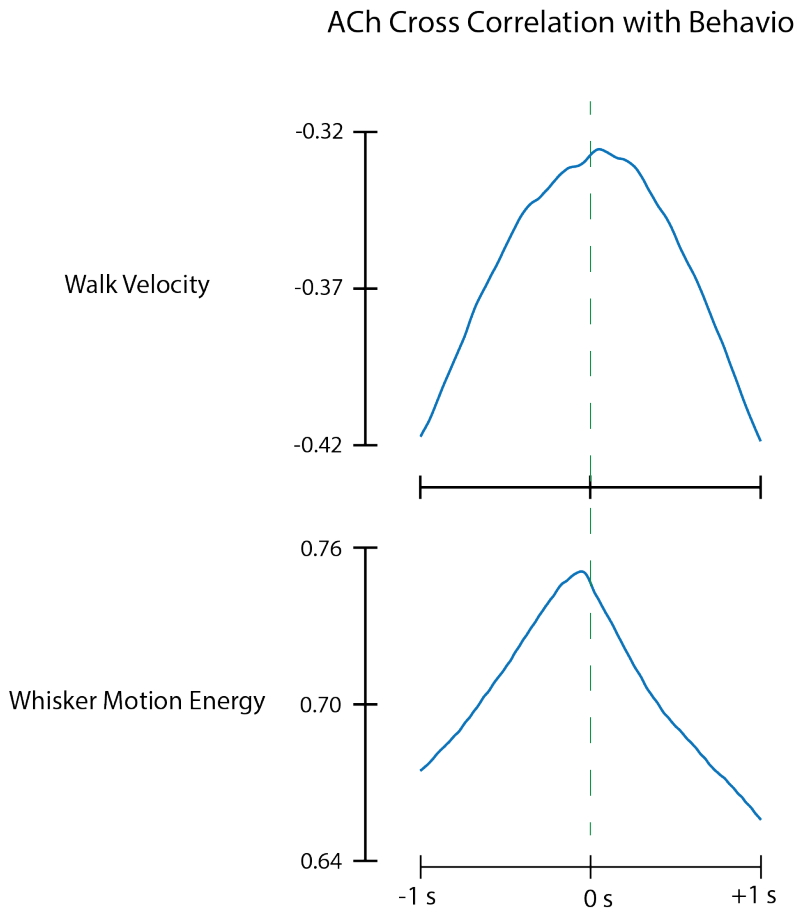

Figure 19. ACh Cross Correlation with Behavior

The peak cross correlation between ACh axonal activity and whisker motion energy and walk velocity are located near 0, when a whisking or walking bout occurred. Peak cross correlation between axonal activity preceded whisking and followed walking activities. The green dashed line indicates timepoint 0. Data were collected from a single ChAT mouse recording session.

Figure 20 shows the peak cross correlation between NA axonal activity and whisker motion energy and walk velocity from a representative example in a single DBH mouse recording session. Changes in NA axon activity slightly preceded changes in whisker pad motion energy, as evidenced by the peak cross correlation between NA

axon activity and whisker pad motion energy being located prior to timepoint 0. Cross correlation between NA axonal activity and whisker pad motion energy peaked after timepoint 0, indicating that NA neuromodulatory activity preceded whisking behavior, but not walking.

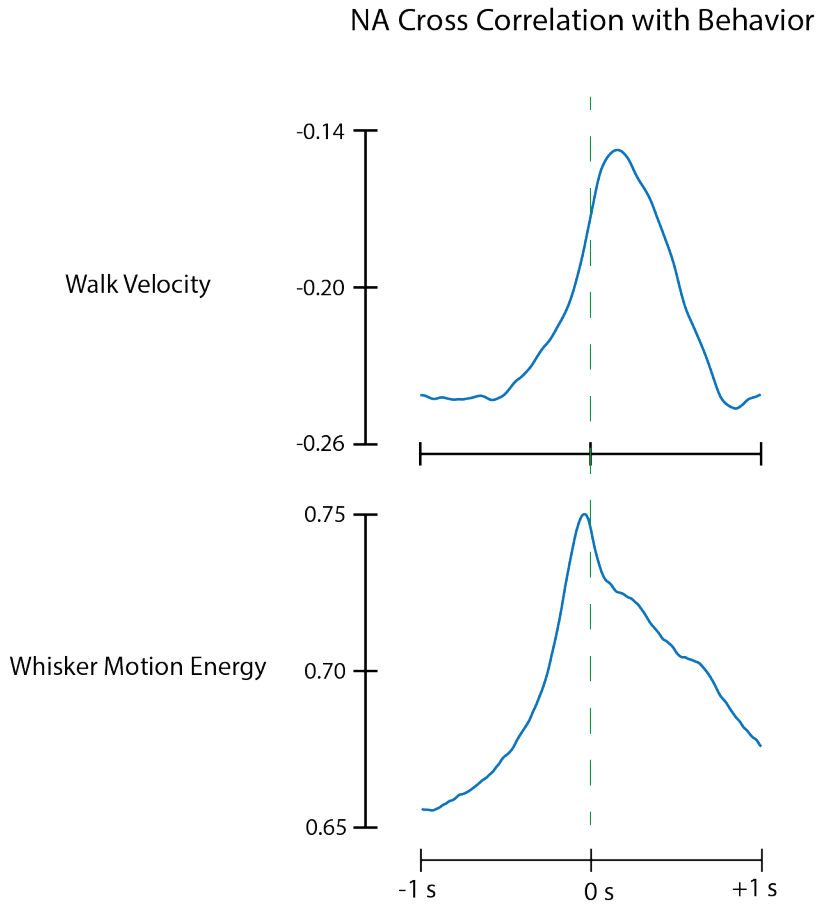

Figure 20. NA Cross Correlation with Behavior

The peak cross correlation between NA axonal activity and whisker motion energy and walk velocity are located at approximately 0, when a whisking or walking bout occurred. Peak cross correlation between axonal activity preceded whisking and followed walking activities. The green dashed line indicates timepoint 0. Data was collected from a single DBH mouse recording session.

To quantitatively determine the temporal differences in cross correlation between neuromodulatory activity and whisking and walking behaviors, the peak cross correlation across all ChAT mice (N = 2) and all respective recording sessions (n = 6) were averaged. These data include 184 axons across 27 ROIs. As seen in Figure 21, the averaged ACh max cross correlation with behavior preceded the onset of whisking and followed the onset of walking. On average, the peak max cross correlation between ACh axonal activity and behavior occurred 0.112 ± 0.0591 seconds prior to the onset of whisking and 0.375 ± 0.247 seconds following the onset of walking. There was a statistically significant difference in the timing between these two peak cross correlation values (Student's t-test; t-statistic = 5.677; $p < 0.01$). The mean max cross correlation between ACh activity and whisking was 0.663 ± 0.085 and between ACh activity and walking was 0.425 ± 0.562. Additionally, there was a statistically significant difference in the average max cross correlation between ACh activity and these two behaviors (Student's t-test; t-statistic = -5.43; $p < 0.0001$). These data show that ACh axonal activity reliably precedes whisking behavior, but not walking behavior and that ACh signaling is more strongly correlated with whisking than walking.

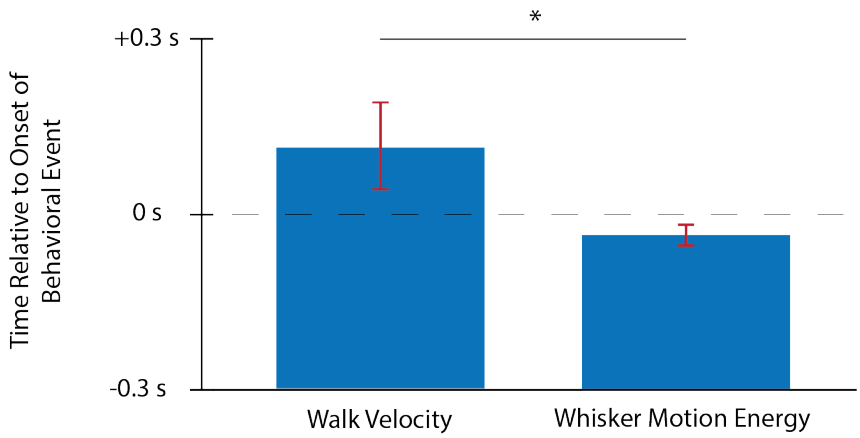

Figure 21. ACh Max Cross Correlation with Behavior

ACh axonal activity reliably preceded whisking behavior and followed walking behavior. Peak cross correlation was averaged across all ChAT recording sessions (n = 6). Data were collected from 184 axons across 27 ROIs. There was a statistically significant difference in the timing between these two peak cross correlation values (t-statistic = 5.677; $p = 0.0013$). * = $p < 0.01$. Error bars indicate standard deviation. Horizontal dashed line indicates onset of behavioral event.

In Figure 22, the peak cross correlation across all DBH mice (N = 3) and all recording sessions (n = 7) were averaged. These data include 94 axons across 24 ROIs. The averaged NA max cross correlation with behavior preceded the onset of whisking and followed the onset of walking. On average, the peak max cross correlation between ACh axonal activity and behavior occurred 0.127 ± 0.0275 seconds before the onset of whisking and 0.869 ± 0.301 seconds following the onset of walking. There was also a statistically significant difference in the timing between these two peak cross correlation values (Student's t-test; t-statistic = 8.175; $p < 0.001$). The mean max cross correlation between NA activity and whisking was 0.696 ± 0.082 and between NA activity and walking was -0.366 ± 0.125. Additionally, there was a statistically significant difference

in the average max cross correlation between NA activity and these two behaviors (Student's t-test; t-statistic = -103.3; $p < 0.0001$). Like the cholinergic neuromodulatory system, these data demonstrate that NA axonal activity reliably precedes whisking behavior, but not walking behavior and that NA signaling is much more strongly correlated with whisking than walking.

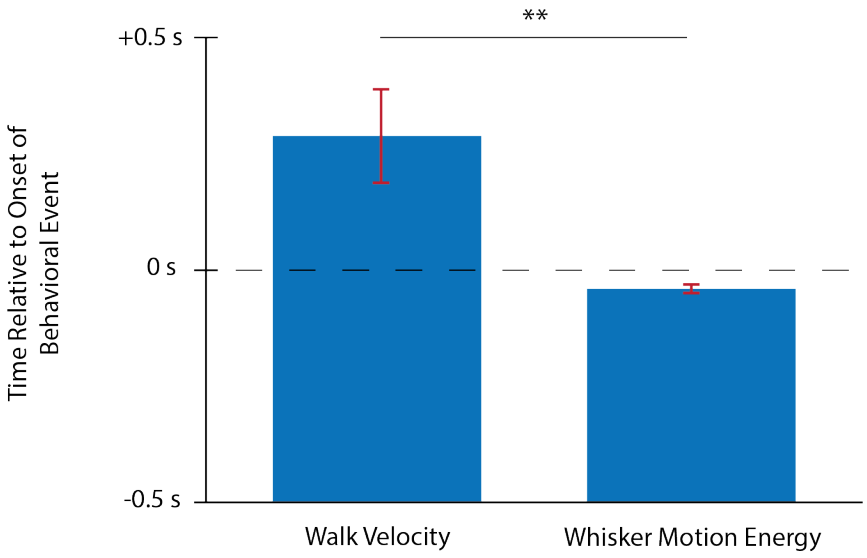

Figure 22. NA Max Cross Correlation with Behavior

NA axonal activity reliably preceded whisking behavior and followed walking behavior. Peak cross correlation was averaged across all DBH mice recording sessions (n = 7). Data were collected from 94 axons across 24 ROIs. There was a statistically significant difference in the timing between these two peak cross correlation values (t-statistic = 8.175 p = 0.00018). ** = $p < 0.001$. Error bars indicate standard deviation. Horizontal dashed line indicates onset of behavioral event.

Analysis of Synchrony Between Cortical Regions During Fluctuating Arousal States

Last, I determined whether there exists global synchrony or localized specificity among groups of ACh or NA axons across the cortex during fluctuating arousal and behavioral states. A 1 second sliding window was used to calculate cross correlations between all pairs of axons over time. The average cross correlation between cortical axons were temporally aligned to the traces of pupil diameter, whisker motion energy, and walk velocity in an example ChAT mouse recording session. Figure 23 shows the average cross correlation between cholinergic axons alongside behavioral measures. As indicated by the dashed, red boxes, increases in walk velocity, whisker motion energy, and pupil diameter were all associated with decreased average cross correlation between cholinergic axons. During bouts of whisking without walking, however, these drastic decreases in average cross correlation did not occur. These data suggest that there exists cortical specificity among cholinergic axons during locomotion.

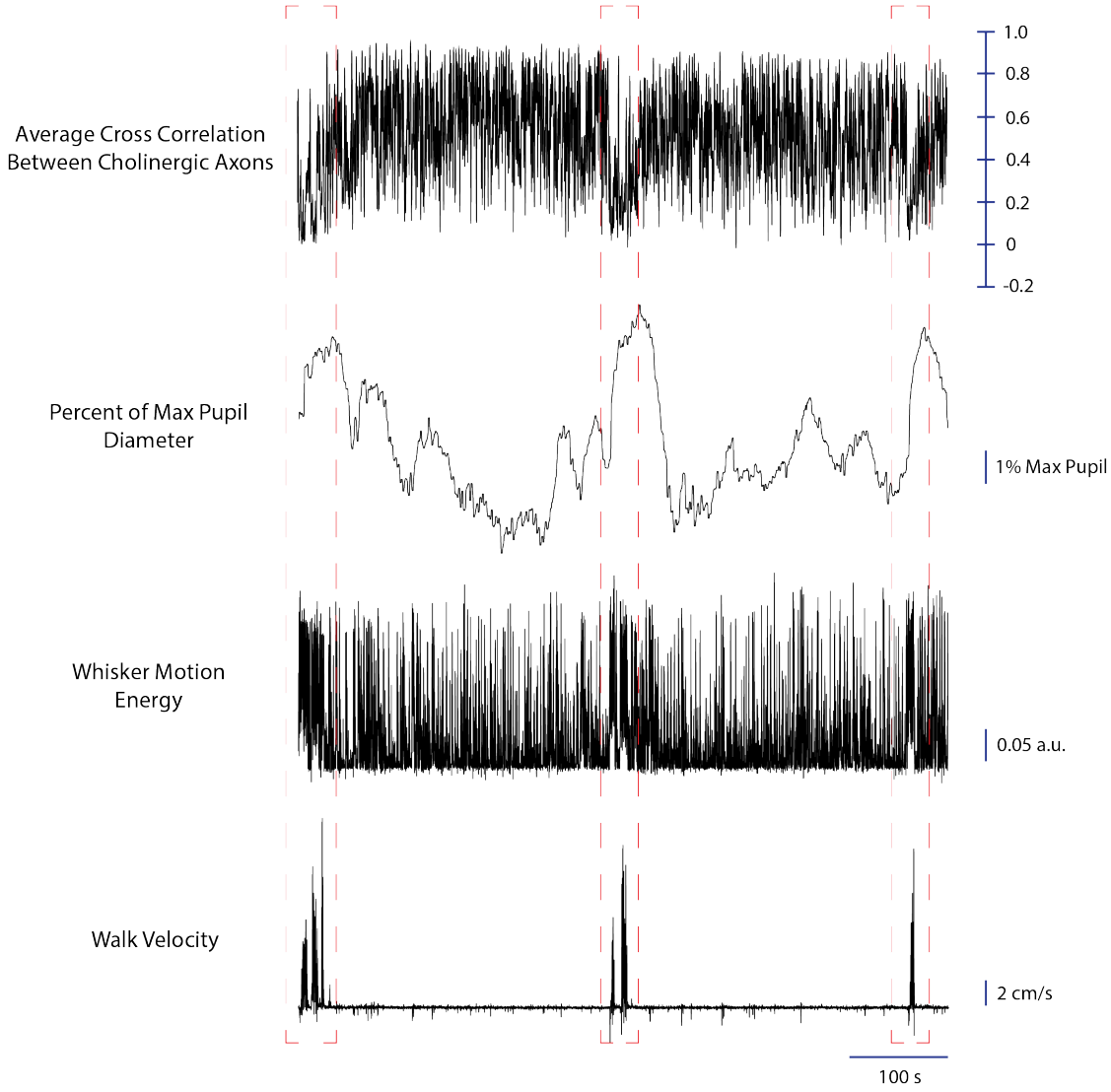

Figure 23. Average Cross Correlation Between Cholinergic Axons Temporally Aligned to Behavior

During walking bouts, there were significant decreases in cross correlation between cholinergic axons across the cortex (dashed red boxes). Data shown from a single representative ChAT mouse recording session.

Similar observations were made when averaging the cross correlation between noradrenergic axons temporally aligned to behavior in DBH mice (example shown in Figure 24). Shown by dashed, red boxes, increases in walk velocity, whisker motion

energy, and pupil diameter were all associated with decreased average cross correlation between noradrenergic axons. Also similar to cholinergic axons, during bouts of whisking without walking, these drastic decreases in average cross correlation did not occur. These data suggest that there exists cortical specificity among noradrenergic axons during locomotion.

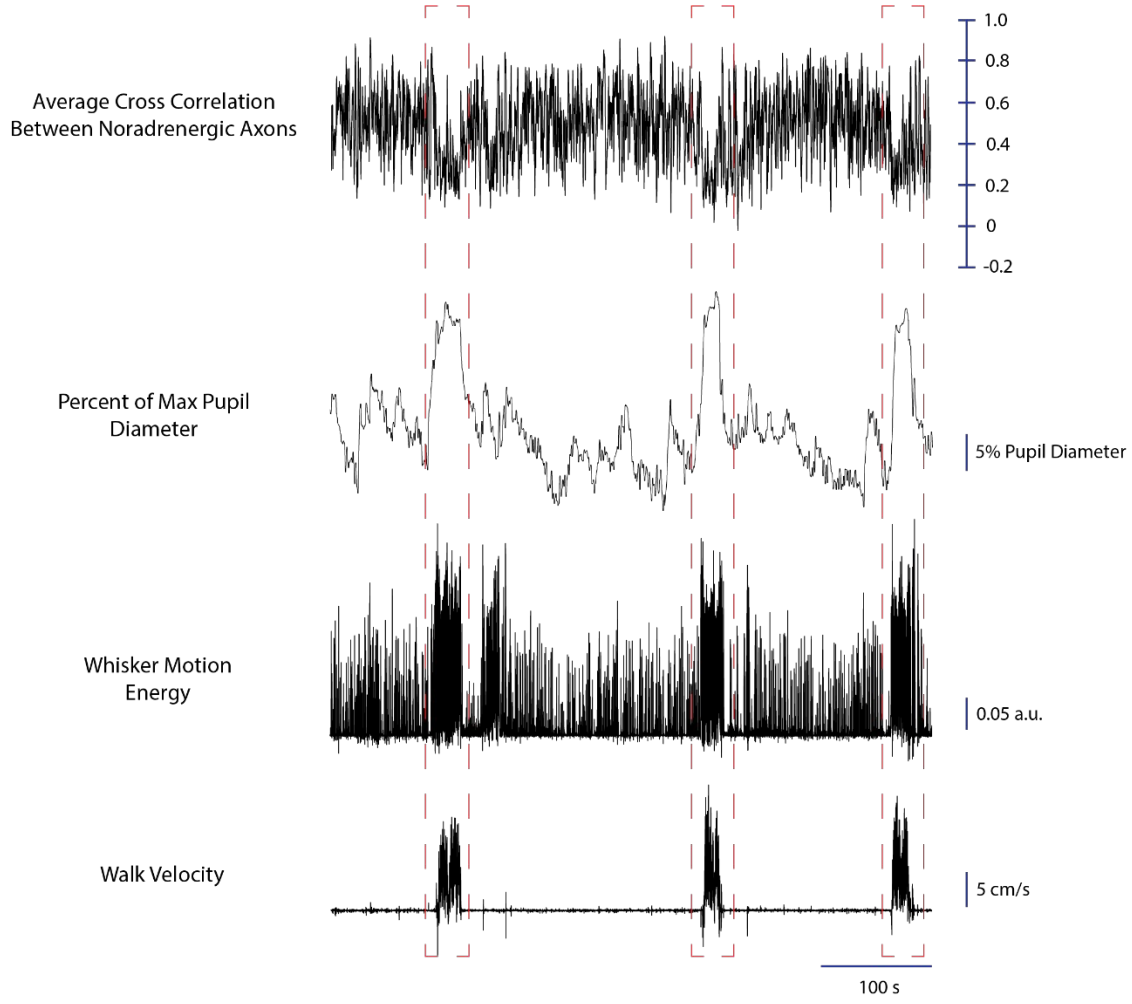

Figure 24. Average Cross Correlation Between Noradrenergic Axons Temporally Aligned to Behavior

During walking bouts (dashed red boxes), there were significant decreases in cross correlation between noradrenergic axons across the cortex. Data shown from a single representative DBH mouse recording session.

To determine the consistency of this relationship between axon-to-axon correlation and behavioral state, the max cross correlation between cholinergic axons for all ChAT mice recording sessions (6 sessions, 27 ROIs, and 184 axons) were averaged for all periods of stillness (neither walking nor whisking), whisking, and walking (Figure 25). On average, the max cross correlation between cholinergic axons was highest during stillness (0.613 ± 0.314), intermediate during whisking (0.500 ± 0.220), and lowest during walking (0.286 ± 0.257; one-way ANOVA; $F = 53.25$; $p < 0.0001$).

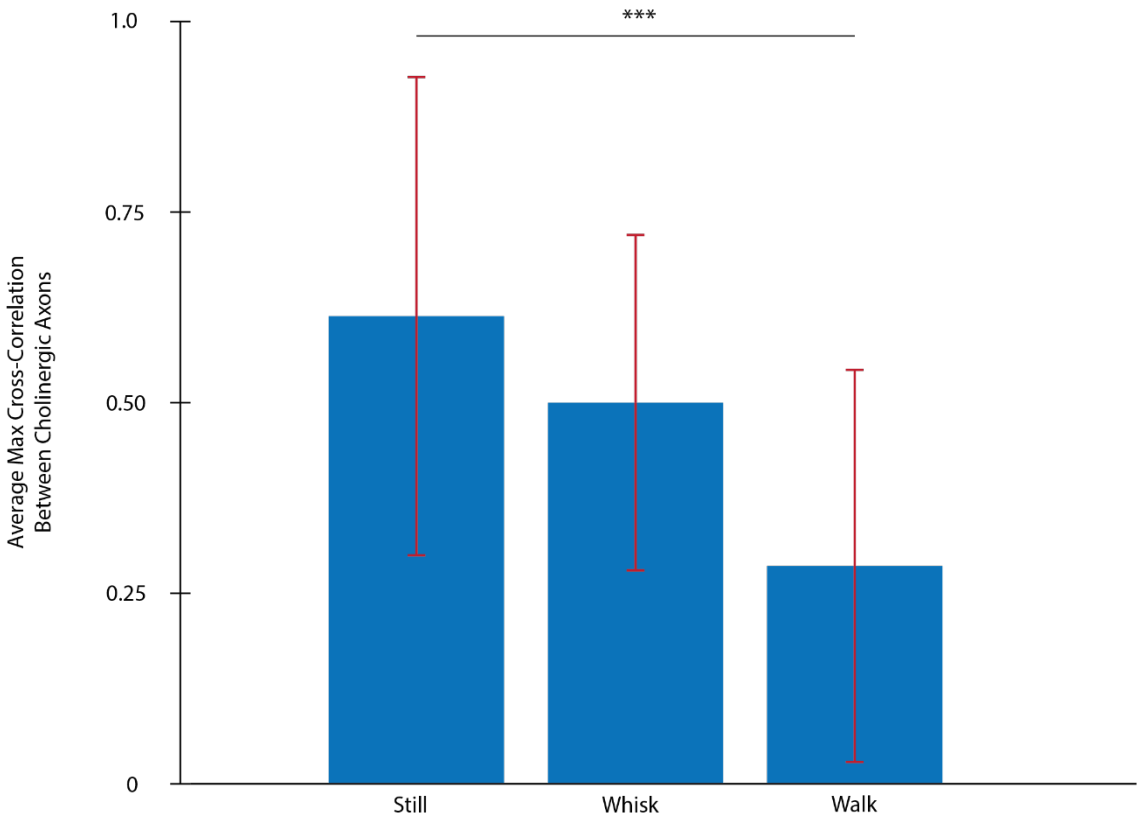

Figure 25. Average Max Cross-Correlation Between Cholinergic Axons during Periods of Stillness (neither walking nor whisking), Whisking, and Walking

Data presented are from all ChAT mice recording sessions (6 sessions, 27 ROIs, and 184 axons). *** = $p < 0.0001$. Error bars indicate standard deviation.

Across all DBH recordings, the max cross correlation between noradrenergic axons did not differ by behavioral state. Max cross correlation was similar during stillness (0.396 ± 0.277), whisking (0.427 ± 0.284), and walking (0.385 ± 0.257; one-way ANOVA; $F = 2.57$; $p > 0.05$).

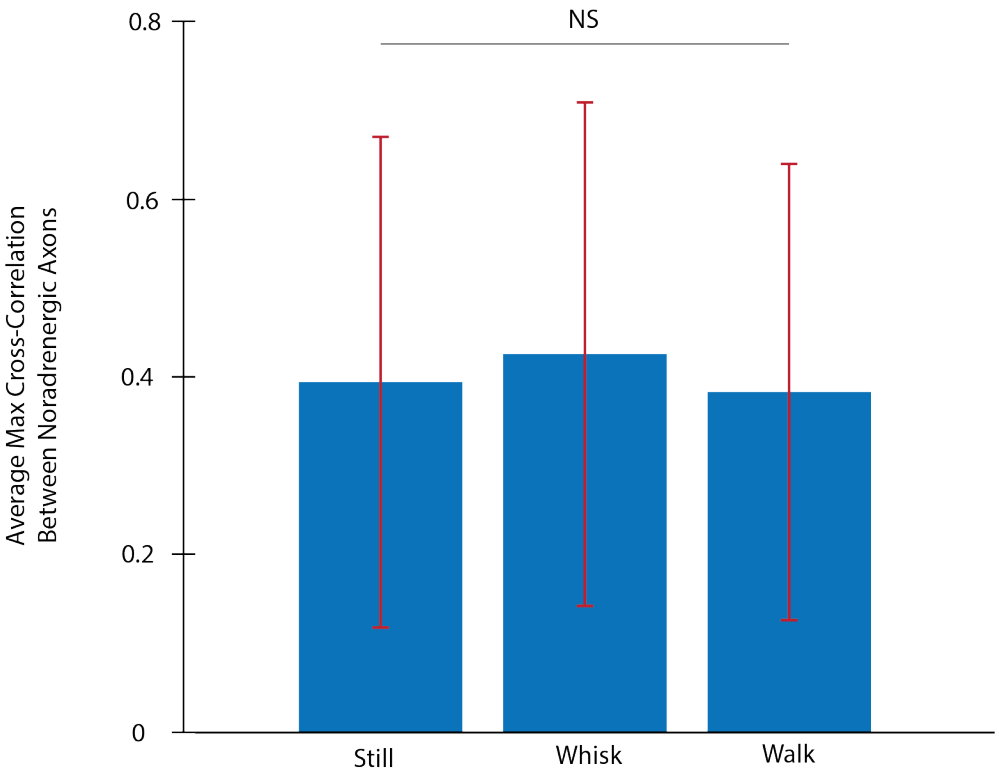

Figure 26. Average Max Cross-Correlation Between Noradrenergic Axons during bouts of Stillness (neither walking, nor whisking), Whisking, and Walking

Data presented are from 3 DBH mice recording sessions (7 sessions, 24 ROIs, and 94 axons). NS = not significant; $p > 0.05$. Error bars indicate standard deviation.

Discussion

This project was designed to investigate the relationship between changes in cholinergic and noradrenergic signaling and observable patterns of behavior in mice. Recent findings show that there exists more regionally-specific and state-dependent modes of cholinergic and noradrenergic neuromodulation (Laszlovszky et al., 2020, Chandler et al., 2019, Obermayer et al., 2017, and Zagha et al., 2014). This differs from earlier models of globally synchronous neuromodulation within the brain (Lee et al., 2012). The present study presents novel data that support the dynamic model of neuromodulatory signaling, particularly in the cholinergic system. Overall, these data offer critical insights that reveal more about how changing neuromodulatory activity interacts with an animal's behavioral state.

First, this project confirmed the previously reported relationship between cholinergic and noradrenergic neuromodulatory activity and behavioral state (McCormick et al., 2020 and Reimer et al., 2016). Two-photon calcium imaging, coupled with simultaneous behavioral video acquisition, confirmed that neuromodulatory axon activity across the cortex did indeed reflect changes in behavioral state. Increases in pupil diameter, whisking, and walking were all accompanied by broad increases in cholinergic and noradrenergic axonal activity across the cortex (Figures 13-14).

Second, this project analyzed the temporal relationship between changes in neuromodulatory activity and the onset and offset of behavioral events. By temporally aligning changes in either cholinergic or noradrenergic fluorescence to the onset and offset of whisking and walking, we showed that ACh and NA activity closely and

reliably tracked the onset, but not the offset, of whisking activity. Further, ACh and NA activity did not track the onset or offset of walking comparatively well (Figures 15-18).

It is interesting to note that when temporally aligning ACh and NA axonal activity to the onset of whisking and walking, pupil diameter seemed to slightly lag drastic increases in whisker motion energy, but not walking velocity (Figures 15-16). This observation can partially be explained by the longer time-scale during which pupillary responses occur. Dilation and constriction of the pupil is controlled by the dilator muscle fibers and sphincter muscle fibers, respectively. These relatively slow-acting smooth muscles controlling the pupil are responsible for the lag observed in changes in pupil diameter (Sghari et al., 2020 and Larsen et al., 2018). We do not see these delayed increases in pupil diameter during the onset of walking since whisking almost always occurs before walking, although whisking is not necessary for walking to occur (McCormick et al., 2020). And so, since the pupil is "primed" and has already started to reflect changes in behavioral state from prior whisking, there is no lag observed in pupil diameter changes during walking.

By calculating the cross correlation between either ACh or NA axonal activity and whisking and walking, we showed that increases in both ACh and NA neuromodulatory activity reliably preceded increases in whisking activity, but not walking behavior (Figures 19-22). These findings are indicative of a strong relationship between cholinergic and noradrenergic neuromodulation and fast arousal changes. A possible explanation for this interesting relationship between neuromodulatory systems and specific behavioral motifs is that behavioral activities that are observed in highly aroused animals, such as whisking or walking, are likely associated with changes in the

state of other physiological processes, such as heart rate and respiration (McCormick et al., 2020). Activation of cholinergic and noradrenergic systems are likely part of a more general arousal system that affects the brain and body and contributes to transitions between arousal states.

Last, this project analyzed synchrony between cortical regions during fluctuating arousal states. To accomplish this, we averaged the cross correlation between either cholinergic or noradrenergic axons across the cortex. This provided a useful measure for the extent to which axons in disparate regions of the cortex were behaving similarly. We found that the cross correlation between cholinergic axons significantly decreased during periods of high arousal. These findings indicate that there exists regional specificity with regard to localized, cholinergic neuromodulation of behavioral activity in a highly aroused animal. However, noradrenergic neuromodulation of these same behaviors exhibited more global synchrony (Figures 23-26). This significant difference between the cholinergic and noradrenergic neuromodulatory systems may be influenced by varying innervation patterns from their respective nuclei to the cortex (Rho et al., 2018). Alternatively, different neuromodulatory systems may be regulating the different needs of an animal as sensory processing occurs. For example, recent work demonstrates that regional neuromodulation may indicate a fine spatial control system as brain state varies (Poulet et. al., 2019).

Identifying the regions of the cortex from which the ROI groupings of axons were recorded was beyond the scope of this project. This limitation in the interpretation of these findings poses new questions that may reveal even more complex and distinct neuromodulatory circuitry underlying behavior. For example, is there any relationship

between the relative distances between ROIs that affects how they temporally activate with respect to one another? Or, do we observe similar relationships found in this study when comparing ROIs from similar or different regions of the cortex that are responsible for controlling distinct aspects of behavior? For example, how do ROIs from the somatosensory cortex, which receives and processes sensory information, behave with respect to ROIs localized to the motor cortex, which is responsible for voluntary motor movements. These findings would be a particularly interesting avenue for further research as previous studies have demonstrated that there exist incredibly interesting dynamic interactions between cortical regions that are behavior and context dependent (Poulet et al., 2019 and Teichet et al., 2018). While identifying the exact cortical regions from which these ROIs were present was beyond the scope of this project, this limitation presents as a promising future direction to better understand the relationship between neuromodulation and multimodal cortical interactions.

Another limitation encountered during this study is that some axons that were recorded within a given ROI may have been projections from the same subcortical neurons. As described in the introduction, a neuron's axon projects from the cell body and branches into axon terminals (Figure 3). However, it is quite difficult to definitively determine whether axonal projections are from distinct neuronal cell bodies. Given the spatial resolution of the two-photon mesoscope used in this study, some axons recorded may have been projections from the same cell bodies. To mitigate this issue, all axonal recordings were manually verified to minimize the possibility of recording from the same cortical neurons. This limitation highlights unique challenges posed by the incredibly diverse and complex morphology of the brain.

To increase our understanding of how neuromodulatory activity is related to behavioral state in mice, future additions to our experimental design include implementing other behavioral motifs into our behavioral analyses. These behaviors include snout movement, facial twitching, grooming, and tail motion. By broadening the amount and types of behavioral activities included in our data set, we could potentially gain a more comprehensive understanding of how cholinergic and noradrenergic signaling are related to incredibly varied behavioral and arousal states. These data would offer valuable insights into how neuromodulation occurs on a behavioral spectrum, rather than being restricted to distinct levels of brain state and arousal. This, in turn, would be more reflective of the mammalian brain.

Identifying the fidelity of neuromodulatory-related axonal activity in relation to observable patterns of behavior is also an interesting avenue of future analyses. That is, understanding the prediction reliability between changes in axonal activity and the onset and offset of behavioral events may be of great interest in understanding state-dependent behavior. These additional analyses would provide us with a better understanding of the extent to which neuromodulation impacts behavior. Further, identifying whether neuromodulatory circuits have any predictive validity with regard to higher-order neural processing, such as learning and memory, is a promising field of research (Barron et al., 2020, Schneider et al., 2020, Kaplan et al., 2020, Avery et al., 2017, and Joshi et al., 2016). Additionally, observing how cholinergic and noradrenergic activity modulates task-dependent behavior while an animal is performing various behavioral assays would provide us with additional insights into these dynamic neuromodulatory systems.

These data lay a foundation for future studies aimed at gaining a better understanding of how behavior is regulated in mammals. While these findings are exclusive to mice, other studies have worked to reveal the intricacies of neuromodulation in non-human primates. (Vijayraghavan et al., 2021 and Zhou et al., 2019). Technological advances in the field of systems neuroscience consistently broadens our ability to eventually bridge the gap between model organisms and humans. For example, given the present validity of pupillometry as an accurate, external metric of brain state, some studies are combining pupillometric data acquisition with steady state blood oxygenation level dependent functional magnetic resonance imaging to understand noradrenergic neuromodulation in humans (DiNuzzo et al., 2019). Because this study confirms neuromodulatory relationships previously found in the literature and offers novel insights into the complex neural circuitry of the mammalian brain, the data provided in this project may potentially be used as a framework for future human studies.

The findings in this project confirm the relationship between neuromodulatory activity and observable patterns of behavior, demonstrate that increases in both ACh and NA axonal activity closely track and precede the onset whisking bouts, but not walking, and show that ACh axonal activity across the cortex is significantly less correlated during whisking and walking compared to stationary periods. In summary, this thesis furthers our current knowledge of the relationship between neuromodulatory activity and observable patterns of behavior by offering new evidence of more localized, state-dependent modes of neuromodulation.

Bibliography

Avery, M. C., & Krichmar, J. L. (2017). Neuromodulatory Systems and Their Interactions: A Review of Models, Theories, and Experiments. *Frontiers in Neural Circuits*, *11*.

Barron, H. C., Auksztulewicz, R., & Friston, K. (2020). Prediction and Memory: A Predictive Coding Account. *Progress in Neurobiology*, *192*.

Chandler, D. J., Jensen, P., McCall, J. G., Pickering, A. E., Schwarz, L. A., & Totah, N. K. (2019). Redefining Noradrenergic Neuromodulation of Behavior: Impacts of a Modular Locus Coeruleus Architecture. *Journal of Neuroscience*, *39*, 8239-8249.

DiNuzzo, M., Mascali, D., Moraschi, M., Bussu, G., Maugeri, L., Mangini, F., Fratini, M., & Giove, F. (2019). Brain Networks Underlying Eye's Pupil Dynamics. *Frontiers in Neuroscience*, *13*.

Gielow, M. R., & Zaborszky, L. (2017). The Input-Output Relationship of the Cholinergic Basal Forebrain. *Cell Reports*, *18*.

Joshi, S., Li, Y., Kalwani, R., & Gold, J. I. (2016). Relationships between Pupil Diameter and Neuronal Activity in the Locus Coeruleus, Colliculi, and Cingulate Cortex. *Neuron*, *89*.

Kaplan, H. S., & Zimmer, M. (2020). Brain-wide Representations of Ongoing Behavior: A Universal Principle? *Current Opinion in Neurobiology*, *64*.

Larsen, R. S., & Waters, J. (2018). Neuromodulatory Correlates of Pupil Dilation. *Frontiers in Neural Circuits*.

Laszlovszky, T., Schlingloff, D., Hegedüs, P., Freund, T. F., Gulyás, A., Kepecs, A., & Hangya, B. (2020). Distinct Synchronization, Cortical Coupling and Behavioral Function of Two Basal Forebrain Cholinergic Neuron Types. *Nature Neuroscience*, *23*, 992-1003.

Lee, S.-H., & Dan, Y. (2012). Neuromodulation of Brain States. *Neuron*, *76*, 209-222.

McCormick, D. A., Nestvogel, D. B., & He, B. J. (2020). Neuromodulation of Brain State and Behavior. *Annual Review of Neuroscience*, *43*, 391-415.

McGinley, M. J., David, S. V., & McCormick, D. A. (2015). Cortical Membrane Potential Signature of Optimal States for Sensory Signal Detection. *Neuron*, *87*, 179-192.

McGinley, M. J., Vinck, M., Reimer, J., Batista-Brito, R., Zagha, E., Cadwell, C. R., Tolias, A. S., Cardin, J. A., & McCormick, D. A. (2015). Waking State: Rapid Variations Modulate Neural and Behavioral Responses. *Neuron*, *87*.

Obermayer, J., Verhoog, M. B., Luchicchi, A., & Mansvelder, H. D. (2017). Cholinergic Modulation of Cortical Microcircuits Is Layer-Specific: Evidence from Rodent, Monkey and Human Brain. *Frontiers in Neural Circuits*, *11*.

Picciotto, M. R., Higley, M. J., & Mineur, Y. S. (2012). Acetylcholine as a Neuromodulator: Cholinergic Signaling Shapes Nervous System Function and Behavior. *Neuron*, *76*.

Reimer, J., McGinley, M. J., Liu, Y., Rodenkirch, C., Wang, Q., McCormick, D. A., & Tolias, A. S. (2016). Pupil Fluctuations Track Rapid Changes in Adrenergic and Cholinergic Activity in Cortex. *Nature Communications*, *7*.

Rho, H.-J., Kim, J.-H., & Lee, S.-H. (2018). Function of Selective Neuromodulatory Projections in the Mammalian Cerebral Cortex: Comparison Between Cholinergic and Noradrenergic Systems. *Frontiers in Neural Circuits*, *12*.

Schneider, D. M. (2020). Reflections of Action in Sensory Cortex. *Current Opinion in Neurobiology*, *64*.

Sghari, S., Davies, W. I. L., & Gunhaga, L. (2020). Elucidation of Cellular Mechanisms That Regulate the Sustained Contraction and Relaxation of the Mammalian Iris. *Investigative Ophthalmology & Visual Science*, *61*.

Sofroniew, N. J., Flickinger, D., King, J., & Svoboda, K. (2016). A Large Field of View Two-Photon Mesoscope with Subcellular Resolution for In Vivo Imaging. *Elife*, *5*.

Teichert, M., & Bolz, J. (2018). How Senses Work Together: Cross-Modal Interactions between Primary Sensory Cortices. *Neural Plasticity*.

Totah, N. K., Neves, R. M., Panzeri, S., Logothetis, N. K., & Eschenko, O. (2018). The Locus Coeruleus Is a Complex and Differentiated Neuromodulatory System. *Neuron*, *99*.

Vijayraghavan, S., & Everling, S. (2021). Neuromodulation of Persistent Activity and Working Memory Circuitry in Primate Prefrontal Cortex by Muscarinic Receptors. *Frontiers in Neural Circuits*, *15*.

Wu, D., Courtney, C. G., Lance, B. J., Narayanan, S. S., Dawson, M. E., Oie, K. S., & Parsons, T. D. (2010). Optimal Arousal Identification and Classification for Affective Computing Using Physiological Signals: Virtual Reality Stroop Task. *IEEE Transactions on Affective Computing*, *1*, 109-118.

Zagha, E., & McCormick, D. A. (2014). Neural Control of Brain State. *Current Opinion in Neurobiology*, *29*.

Zhou, A., Santacruz, S. R., Johnson, B. C., Alexandrov, G., Moin, A., Burghardt, F. L., Rabaey, J. M., Carmena, J. M., & Muller, R. (2019). A Wireless and Artefact-free 128-channel Neuromodulation Device for Closed-loop Stimulation and Recording in Non-human Primates. *Nature Biomedical Engineering*, *3*.